π Conjugation Across the Tetrathiafulvalene Core: Synthesis of Extended Tetrathiafulvalene Derivatives and Theoretical Analysis of their Unusual Electrochemical Properties

Najoua Terkia-Derdra,[a, e] Raquel Andreu,[b] Marc Sallé,*[a] Eric Levillain,*[a] Jesús Orduna,[b] Javier Garín,*[b] Enrique Ortí,*[c] Rafael Viruela,[c] Rosendo Pou-Amérigo,[c] Bouchta Sahraoui,[d] Alain Gorgues,[a] Jean-François Favard,[a] and Amédée Riou[a]

Abstract: A series of extended tetrathiafulvalene (TTF) derivatives bearing one or two 1,4-dithiafulven-6-yl substituents has been prepared. The new compounds present remarkable electrochemical singularities compared with other TTF derivatives, which are strongly affected by the nature of the substitution on the lateral heterocycle(s). This unusual electrochemical behaviour follows a square-scheme sequence and is attributed to structural changes upon oxidation of the π-donating molecules. Digital simulations of the electrochemical data have been used to reach the values of the kinetic and thermodynamic constants involved in the square scheme. Theoretical calculations establish an important contribution of a highly delocalised resonant form involving a tetravalent sulphur in oxidised species, which could justify the occurrence of an electrochemical behaviour distinct from that of TTF. Finally, third-order susceptibilities χ^3 of two of these systems, for which electron-donating and electron-withdrawing substituents coexist and are conjugated through the TTF π system, are given.

Keywords: ab initio calculations · cyclic voltammetry · nonlinear optics · tetravalent sulfur · tetrathiafulvalene

Introduction

A substantial amount of work is devoted in the field of organic conductors and superconductors to the search of new π-donor molecules prone to generate two-dimensional networks when forming radical-cation salts. Such a dimensionality is a requirement to promote the stabilisation of the metallic state down to low temperatures.[1] In this respect, (electro)oxidation of the sulphur-rich bis(ethylenedithio)tetrathiafulvalene (BEDT-TF) has generated a wide variety of two-dimensional arrays, some of them displaying a superconducting behaviour.[1, 2]

We have recently shown that highly extended, sulphur-rich tetrathiafulvalene (TTF) derivatives obtained from di- or tetrasubstitution of the TTF core with *1,4-dithiafulven-6-yl* fragments (e.g., compound **I**) can lead to original two-dimensional associations in the corresponding electrogenerated radical-cation salts.[3] The most noticeable electrochemical features of these π-systems are: i) their propensity to substantially enhance the π-donating ability of TTF, which is promoted by the electron-donating conjugated 1,4-dithiaful-

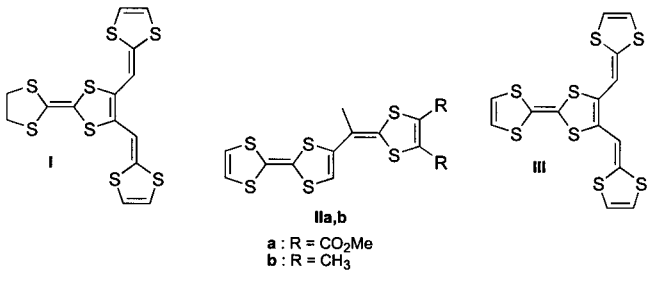

[a] Prof. M. Sallé, Dr. E. Levillain, Dr. N. Terkia-Derdra, Prof. A. Gorgues, Dr. J.-F. Favard, Prof. A. Riou
Laboratoire d'Ingénierie Moléculaire et Matériaux Organiques, UMR CNRS 6501
Université d'Angers, 2 Bd Lavoisier, 49045 Angers (France)
Fax: (+33) 2-41-73-54-05
E-mail: salle@univ-angers.fr

[b] Prof. J. Garín, Dr. R. Andreu, Dr. J. Orduna
Instituto de Ciencia de Materiales de Aragón
Unidad de Nuevos Materiales Orgánicos, Facultad de Ciencias
CSIC-Universidad de Zaragoza, 50009 Zaragoza (Spain)

[c] Prof. E. Ortí, Prof. R. Viruela, Dr. R. Pou-Amérigo
Departamento de Química Física
Universidad de Valencia, Dr Moliner 50
46100 Burjassot, Valencia (Spain)

[d] Dr. B. Sahraoui
Laboratoire des Propriétés Optiques des Matériaux et Applications, Université d'Angers
2 Bd Lavoisier, 49045 Angers (France)

[e] Dr. N. Terkia-Derdra
Laboratoire de Synthèse Organique Appliquée
Université d'Oran, Es-Sénia, BP 1524 Oran (Algeria)

 © WILEY-VCH Verlag GmbH, D-69451 Weinheim, 2000 0947-6539/00/0607-1199 $ 17.50+.50/0

ven-6-yl substituents, and ii) their capability to form stable multicharged species, which are easily reached upon oxidation thanks to the lowering of coulombic repulsions.[4] Furthermore, their planar and highly extended molecular structure, associated with the multiplication of S atoms, provide a unique opportunity for efficient overlapping in the solid state. These structural features are actually restored in the solid state for the $\mathbf{I}^{\cdot+}ClO_4^-$ radical-cation salt, and justify the high room-temperature conductivity ($0.38\,S\,cm^{-1}$) though no mixed valency is present in this salt.[3]

Moreover, a few papers have been recently devoted to the use of the TTF unit as the donor part in (donor–π–acceptor) nonlinear optics (NLO) chromophores.[5] The search for new insights about π conjugation through the TTF core therefore appears to be of prime interest.

This paper deals with the synthesis of new planar, highly extended TTF derivatives incorporating one or two electron-donating (D) 1,4-dithiafulven-6-yl substituents in non-vicinal positions. The very unusual electrochemical behaviour of some of these compounds is carefully investigated and is discussed on the basis of theoretical calculations. Furthermore, introduction of electron-withdrawing groups (A) (CN, CO_2Et) on these extended TTF derivatives has also been performed in order to further explore π conjugation across the TTF core.

Abstract in French: *Une famille de dérivés étendus du tétrathiafulvalène (TTF) porteurs d'un ou de deux groupements 1,4-dithiafulven-6-yl a été préparée. En fonction de la nature de la substitution sur l'hétérocycle latéral, certains de ces composés présentent des comportements électrochimiques différents de ceux habituellement rencontrés pour les dérivés du TTF. Ce comportement inhabituel obéit à un schéma carré et est attribué à des changements structuraux intervenant lors de l'oxydation du donneur-π. Les données électrochimiques ont été exploitées par simulation afin d'atteindre les constantes cinétiques et thermodynamiques mises en jeu dans le schéma carré. Des calculs théoriques mettent en évidence la contribution importante d'une forme résonante impliquant un atome de soufre tétravalent dans les espèces oxydées, qui pourrait justifier le comportement électrochimique original de ces composés. Enfin, on donne les susceptibilités de troisième ordre χ^3 de deux de ces molécules dans lesquelles des groupements électrodonneurs et électroattracteurs sont conjugués au travers du système-π TTF.*

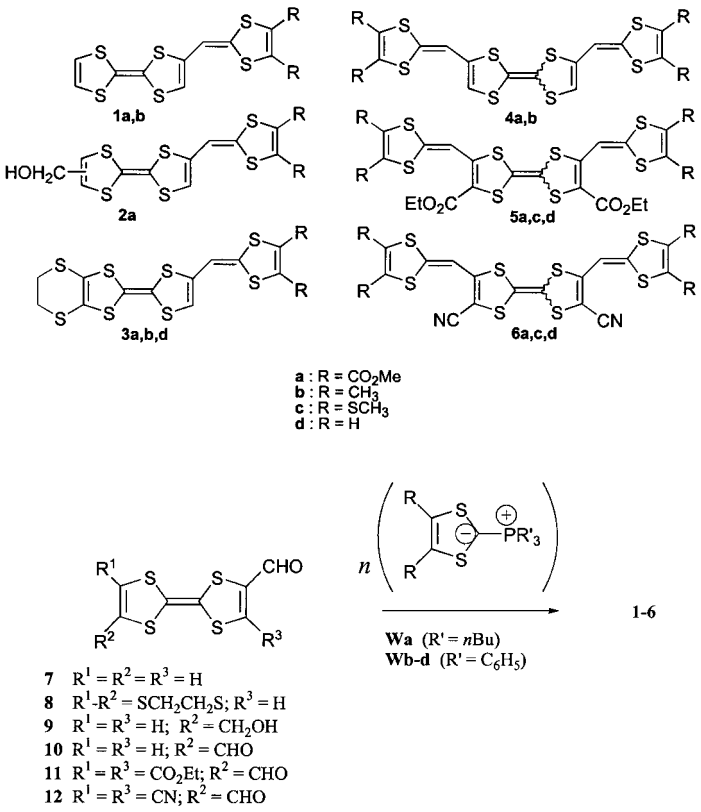

Scheme 1. Reaction scheme for the preparation of compounds **1**–**6**.

Results and Discussion

Synthesis: The general synthetic methodology used to reach the target compounds **1**–**6** involves a Wittig olefination between TTF derivatives **7**–**12** bearing one or two aldehyde functionalities and the P reagents **Wa**[6] or **Wb**–**d**[7] incorporating the 1,3-dithiol-2-ylidene moiety (Scheme 1). This strategy therefore requires the preliminary synthesis of the (poly)formyl-TTF derivatives **7**–**12**.

The monosubstituted derivatives **7** and **8** were synthesised according to the standard methodology, involving lithiation (LDA/THF/$-78\,^\circ C$) and subsequent formylation (with Ph(Me)NCHO) of TTF[8] and (ethylenedithio)tetrathiafulvalene (EDT-TTF),[9] respectively. By analogy with previous reports on the corresponding dioxidation,[10] the synthetic intermediate **9** was obtained in a 40% yield by partial oxidation of 2,6(7)-bis(hydroxymethyl)TTF with one equivalent of selenium dioxide in refluxing dioxane (Scheme 2).

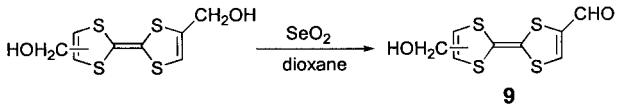

Scheme 2. Reaction scheme for the preparation of compound **9**.

Various pathways to 2,6-bis(formylated)-TTF derivatives **10** have been described recently.[10] We propose here an alternative route, through the formation of an iron-carbene complex. Surprisingly, though this strategy has been explored for the synthesis of various TTF derivatives twenty years ago,[11] very few TTF synthesis that make use of this straightforward methodology have been described.[12] Electrophilic alkynes (R^1-C≡C-R^2) bearing at least one electron-withdrawing R^1 or R^2 substituent are known to add readily to the activated carbon disulphide ligand of the [Fe(η^2-CS_2)$(CO)_2(PPh_3)_2$] complex,[13] to afford stable (1,3-dithiol-2-ylidene)-iron complexes (Scheme 3). The latter are then converted in the corresponding TTF derivatives upon oxidation with iodine or by thermolysis.

© WILEY-VCH Verlag GmbH, D-69451 Weinheim, 2000
0947-6539/00/0607-1200 $ 17.50+.50/0 *Chem. Eur. J.* **2000**, *6*, No. 7

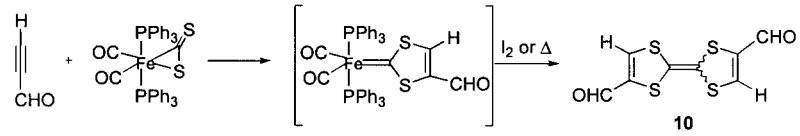

Scheme 3. Reaction scheme for the preparation of compound **10**.

We have used this straightforward strategy to reach the target dialdehyde **10**, by starting from the readily available η^2-CS_2-iron complex and propargylic aldehyde ($R^1 = H$, $R^2 =$ CHO). This aldehyde was generated through treatment of the corresponding di(ethyl)acetal[14] with an excess of formic acid (previously dried over $CuSO_4$), the course of the formolysis being monitored by ^1H NMR spectroscopy. Because of its propensity to explode,[14b] propargyl aldehyde was not isolated in the pure state but in the presence of ethyl formiate thanks to a direct distillation of the reaction mixture ($bp_{(0.9)} = 55-56\,^\circ C$). The distillate was then directly treated with the η^2-CS_2-iron complex (Scheme 3) in toluene, to instantaneously afford the intermediate black (1,3-dithiol-2-ylidene)-iron complex. When immediately treated with iodine, this complex converted to the desired 2,6(7)-diformyl TTF **10**, isolated in a 18% overall yield from propargyl aldehyde. It should be stressed that this route involves a one-pot synthesis from propargyl aldehyde, instead of the long three-step procedure usually carried out to get **10**.[10] In this respect, this strategy proves to be an efficient alternative towards the synthesis of compound **10**.

The still unknown diformyl TTF derivatives **11** and **12** were synthesised according to the classical multistep procedure involving isolation of the 1,3-dithiole-2-thione intermediates **16** and **17** (Scheme 4). Given their powerful synthetic applicability, such new S-heterocycles are of interest in various fields of organic chemistry, and especially as key intermediates to reach TTF derivatives.[15] Thiones **16** and **17** are precursors of TTF derivatives bearing both electron-attracting (CN or CO_2Et) and electron-donating groups (these are formed through olefination of the CHO functionalisation with electron-rich substituents). The occurrence of a two-dimensional conjugation in such TTF derivatives bearing electron-attracting and electron-donating groups should promote the generation of large second- or third-order nonlinear optical responses.[16]

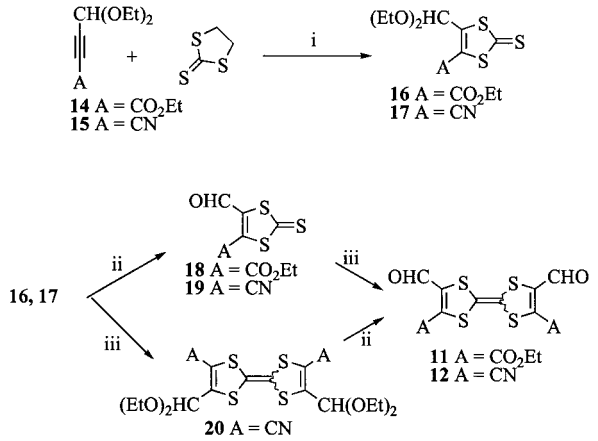

Scheme 4. i) xylene; ii) HCO_2H/CH_2Cl_2; iii) $Co_2(CO)_8$/toluene.

Thiones **16** and **17** were prepared through cycloaddition of electrophilic alkynes **14** and **15** onto ethylenetrithiocarbonate with ethylene evolution. Acetylenic starting products were synthesised by lithiation of propargyl aldehyde diethylacetal and subsequent treatment with ethylchloroformiate or phenyl cyanate, respectively.[17] Compounds **16** and **17**, obtained as oils, were purified by chromatography over silicagel (yields: 54 and 78%, respectively). They undergo a formolysis reaction upon treatment with pure formic acid, giving rise to the free aldehydes **18** and **19**, obtained as yellow orange needles after chromatography and recrystallization (yields: 88 and 50%, respectively) (Scheme 4).

Desulphurizing coupling of 1,3-dithiol-2-thiones **16**–**19** to functionalised TTF derivatives was achieved by using dicobaltoctacarbonyl in refluxing toluene,[18] instead of the more classical phosphine- or phosphite-mediated self-coupling procedure.[15] Indeed, aldehyde functionalised thiones have been shown to react through their carbonyl carbon atom with P reagents to undergo formation of undesirable side products.[19] Hence, a mixture of the *Z* and *E* isomers of the dicarboethoxy derivative **11** were obtained by self-coupling of thione **18** in a 63% yield; the progress of the reaction was monitored by TLC with distinctive R_f values for both blue isomers. Starting from the cyano derivative **19**, we were unable to separate the sparingly soluble coupling product from the organometallic residue. Therefore, the coupling step was performed from the acetalised thione **17**, affording the more soluble TTF derivative **20** in a 21% yield. The diformyl dicyano compound **12** was then quantitatively obtained by formolysis of acetal functions of **20**.

The synthesis of the target extended analogues of TTF **1**[20] and **2**–**6** was carried out through Wittig mono- or diolefinations of aldehydes **7**–**12** with adequate 4,5-disubstituted-1,3-dithiol-2-ylidene P reagents **Wa-d**[6, 7] (Scheme 1); yields were good (53–90%) even in the case of twofold Wittig olefinations. It has to be pointed out that a wide variety of R substituents is available for **W**, so that one may easily increase either the solubility or the π-donating ability (or both of them) of the target molecules. Despite the low solubility of some of these compounds, all of them were characterised by means of usual techniques.

Electrochemistry: The π-donating ability of the new extended donor molecules **1**–**6** has been first evaluated by cyclic voltammetry under standard conditions (scan rate 100 mV s^{-1}), oxidation (E_{ox}) and reduction (E_{red}) potential values are given in Table 1.

All of the monosubstituted TTF systems **1**–**3** exhibit two redox systems at potential values lower than 1.00 V versus SCE with, in some cases, additional redox processes observed at higher potentials.

Compounds **1a**, **2a** and **3a**, whose external dithiafulvenyl ring is substituted with electro-attracting carbomethoxy groups, present the classical electrochemical features of TTF derivatives, characterised by two reversible one-electron

Table 1. Oxidation (E^i_{ox}) and reduction (E^i_{red}) potentials for compounds **1**–**6**.[a]

	1a	**1b**	**2a**	**3a**	**3b**	**3d**	**4a**	**4b**	**5a**	**5c**	**5d**	**6a**	**6c**	**6d**[b]
E^1_{ox}	0.42	0.24	0.38	0.44	0.27	0.33	0.40	0.17	0.57	0.49	0.42	0.85	0.73	–
E^1_{red}	0.32	−0.31	0.31	0.37	−0.28	−0.28	0.33	−0.27	0.49	0.41	0.36	0.79	0.67	–
E^2_{ox}	0.88	0.95	0.82	0.85	0.92	0.96	0.81	0.27	0.93	0.83	0.53	1.13	0.95	–
E^2_{red}	0.77	0.77	0.76	0.77	0.78	0.68	0.72	0.20	0.87	0.77	0.47	1.07	–	–
E^3_{ox}	1.64	–	–	–	1.34	1.33	–	0.82	–	1.30	0.82	–	–	–

[a] $c = 10^{-3}$ mol L^{-1}; potentials vs. SCE in CH_2Cl_2; nBu$_4$NPF$_6$ (0.1 mol L^{-1}); scan rate: 100 mV s^{-1}. [b] Insoluble compound.

oxidation waves (Figure 1) with, in the case of **1a**, detection of a third irreversible oxidation peak at higher anodic potential (1.64 V vs. SCE). The potential values of the two reversible oxidation steps are very close to those of parent TTF systems, namely unsubstituted TTF, hydroxymethyl-TTF and ethylenedisulfanyl-TTF. The first two reversible redox processes

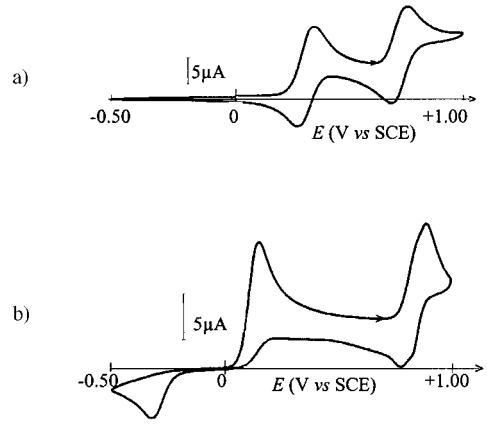

Figure 1. Cyclic voltammetry of a) compound **1a** (3.8×10^{-3} mol L^{-1}) and b) compound **1b** (4.8×10^{-3} mol L^{-1}) in a CH_2Cl_2/CH_3CN (4:1, v/v) mixture; Bu$_4$NPF$_6$ (0.1 mol L^{-1}); 100 mV s^{-1}; 20 °C.

displayed by **1a**, **2a** and **3a** can be therefore assigned to the oxidation of the TTF core into radical-cation and dication states, respectively (Scheme 5). The lack of enhancement of the π-donating ability in **1a**, **2a** and **3a**, relative to the parent

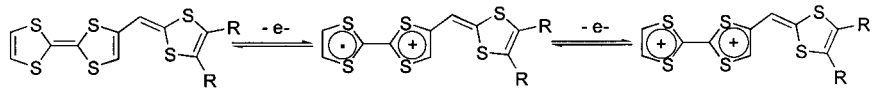

Scheme 5. R = CO_2CH_3.

systems, is an indication of the poor contribution of the lateral dithiafulvenyl substituent and contrasts with the observations made on vicinal bis-substituted dithiafulvenyl TTFs like compounds **I** and **III**.[3]

Voltammograms of compounds **1b**, **3b** and **3d** display two redox systems below 1.00 V in methylene chloride, and a third irreversible process is detected around 1.3 V for **3b** and **3d**. The electrochemical behaviour of these compounds, however, presents remarkable singularities compared with their carbomethoxy analogues (see Table 1 and Figure 1). First, the π-donating ability of **1b**, **3b** and **3d** is markedly stronger than for **1a** and **3a**, in accord with the strengthened electron-donating character of the dithiafulvenyl substituent, bearing in this case H atoms (**3d**) or electron-releasing methyl groups (**1b**, **3b**) (**1b**: $E^1_{ox} = 0.24$ V; **3b**: 0.27 V; **3d**: 0.33 V). This finding suggests that the dithiafulvenyl substituent now contributes to the oxidation process. Second, the first two oxidation processes are separated by 0.6–0.7 V, a potential difference ($E^2_{ox} - E^1_{ox}$) significantly larger than that found for **1a**, **2a** and **3a**, and for TTF itself (≈0.4 V). Third, though their second redox system E^2_{ox}/E^2_{red} appears to be quasi reversible, the reduction peak E^1_{red} corresponding to the first redox system (E^1_{ox}/E^1_{red}) is found at a far lower potential than expected for an electrochemically reversible system ($\Delta E = E^1_{ox} - E^1_{red} = 550-610$ mV). This electrochemical irreversibility is not detected for the **a** series under those experimental conditions, and was neither observed for extended TTFs like **I** and **III**, whatever the substituents on the lateral dithiafulvenyl rings are.[3]

Scanning voltammograms of **1b**, **3b** and **3d** from 0.00 to 0.50 V allowed the observation of the first oxidation peak ($E^1_{ox} = 0.24/0.33$ V vs. SCE) corresponding to formation of the radical-cation state. When reversing the scan from +0.50 to −0.50 V, a reduction peak appears at a very negative potential value ($E^1_{red} = -0.31/-0.28$ V). No detectable change in the shape of the voltammograms is observed when a continuous cycling between −0.50 and +0.50 V is performed. Moreover, a negative sweeping from 0.00 V does not allow detection of any electrochemical response, which indicates that the electrochemical processes corresponding to E^1_{ox} and E^1_{red} are associated. Considering this behaviour, we may assume that E^1_{red} corresponds to the reduction of the radical-cation to the neutral state. This observation is confirmed by a UV-visible spectroelectrochemistry experiment of compound **1b** in thin-layer conditions. Figure 2 shows the evolution of the optical spectrum of this compound during the potential scan at low scan rate. The spectroelectrochemical curves clearly show the development of the characteristic spectral features of a radical-cation TTF derivative[21a–c] in the visible region at 425 and 625 nm when the potential reaches the first anodic peak (E^1_{ox}). It is worth noting that the spectroscopic signature of the radical-cation species is maintained during the backward scan till the cathodic peak is reached (E^1_{red}), at which the spectral features of neutral **1b** appear.

Finally, it has also to be pointed out that:

1) The differences in the electrochemical features between the **a** and **b** families are observed in various solvents (CH_2Cl_2, THF and DMF) and without concentration

 © WILEY-VCH Verlag GmbH, D-69451 Weinheim, 2000 0947-6539/00/0607-1202 $ 17.50+.50/0 *Chem. Eur. J.* **2000**, *6*, No. 7

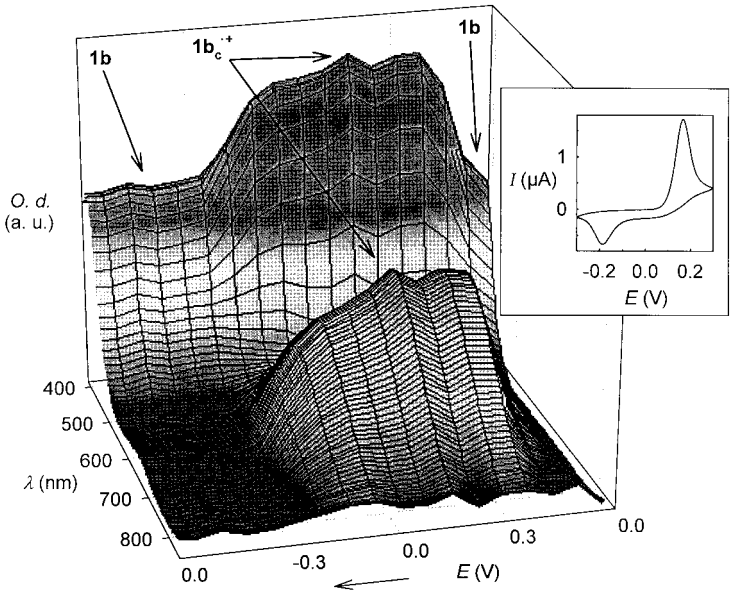

Figure 2. UV-visible spectroelectrochemistry in thin-layer conditions ($d \approx 50\,\mu m$) for **1b**; $c = 3.1 \times 10^{-3}\,mol\,L^{-1}$ in $5 \times 10^{-1}\,mol\,L^{-1}$ TBAHP/ACN/CH_2Cl_2; scan rate 1 mV s^{-1}; reference electrode Ag/AgCl.

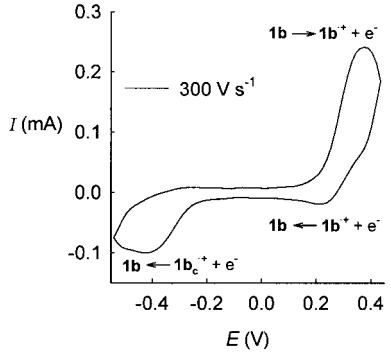

Figure 3. Experimental cyclic voltammogram for **1b** ($3.1 \times 10^{-3}\,mol\,L^{-1}$), 300 V s^{-1}, at 293 K, in $5 \times 10^{-1}\,mol\,L^{-1}$ TBAHP/ACN/CH_2Cl_2, reference electrode Ag/AgCl.

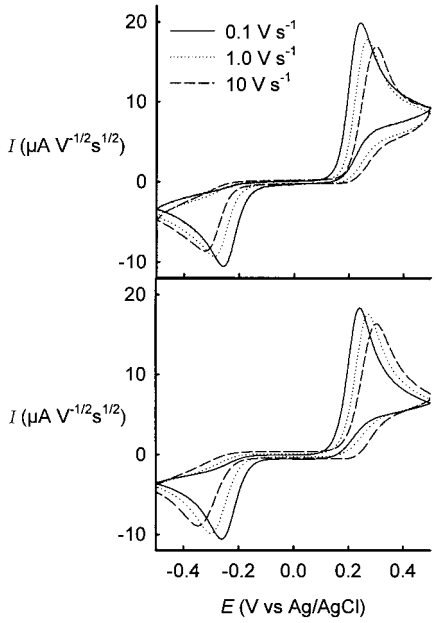

Figure 4. Experimental (top) and simulated (bottom) cyclic voltammograms of compound **1b**. The simulated data (DIGISIM 2.1®) were fitted to experimental results for **1b** ($3.1 \times 10^{-3}\,mol\,L^{-1}$ and $3.1 \times 10^{-4}\,mol\,L^{-1}$) at 293 K according to Scheme 6. All simulations were carried out with the same set of parameters, only the scan rate changed according to the experimental voltammograms (10, 5, 2, 1, 0.5, 0.2 and 0.1 V s^{-1}). For clarity reasons, only three among seven scan rates are represented for $c = 3.1 \times 10^{-3}\,mol\,L^{-1}$. Charge transfer parameters: $E = 0.268$ V vs. Ag/AgCl, $E_c = -0.348$ V vs. Ag/AgCl, $k_s = 0.1\,cm\,s^{-1}$, $\alpha = 0.5$. Chemical reaction parameters: $K_0 = 10^8$, $k_{0f} = 5 \times 10^4\,s^{-1}$ and $K_1 = 4 \times 10^2$, $k_{1f} = 2 \times 10^2\,s^{-1}$. Diffusion coefficient: $D = 8.7 \times 10^{-6}\,cm^2\,s^{-1}$.

dependence, which confirms the occurrence of an intrinsic phenomenon directly associated to the π-donor structure. The concentration independence of voltammetric signals constitutes a good evidence that the charge transfer is followed by a first-order reaction rather than a dimerization process.[21] Moreover, the dimerization of TTF has been discussed in the literature[21a–c] and it is known that the absorption band of TTF dimers appears around 800 nm. For compounds **1a** and **1b**, no absorption band is observed in this region by spectroelectrochemical experiments: the optical spectra show only absorption bands unequivocally assigned to the radical cation.

2) π-donors **IIa** and **IIb**, bearing a methyl substituent on the 6-position of the lateral dithiafulven-6-yl group and synthesised according to ref. [20], exhibit the same electrochemical behaviour as that of their non-methylated analogues **1a** and **1b**, respectively, which excludes a deprotonation process as observed during oxidation in other families of π-donor molecules.[22]

In order to go further into the rationalisation of this unusual electrochemical behaviour, we carefully studied **1b** as a representative compound of the series by performing a voltammetry study versus scan rate. On the one hand, some electrochemical reversibility of the first one-electron oxidation (E^1_{ox}) process of **1b** begins to be observed at high scan rates (> 100 V s^{-1}) (Figure 3). On the other hand, this process appears fully irreversible at low scan rates (Figure 4, top).

Such features are typical of a square-scheme electrochemical sequence as depicted in Scheme 6, and therefore a new redox couple, denoted as ($\mathbf{1b_c}^{\cdot+}/\mathbf{1b_c}$), has to be considered as well as $\mathbf{1b}^{\cdot+}/\mathbf{1b}$. Though no firm evidence of the molecular structure of $\mathbf{1b_c}^{\cdot+}$ can be given, this species may be assigned to a peculiar, highly delocalised, stabilised structural evolution of $\mathbf{1b}^{\cdot+}$ (see theoretical part).

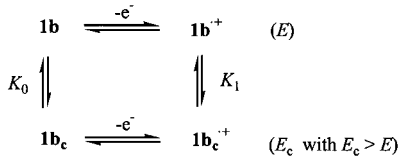

Scheme 6. (E) and (E_c): redox potentials of compounds **1b** and $\mathbf{1b_c}$, respectively.

A quantitative analysis of the data over the scan-rate range investigated was carried out with the aid of digital simulation [DIGISIM 2.1® simulation program (BAS)]. The results of a square-scheme simulation for compound **1b** are shown in

Figure 4 (bottom). The fit involves scan rate changes over two decades ($0.1-10\,V\,s^{-1}$) and uses one set of simulation parameters. An excellent agreement between experiment and simulation is found.

Very interestingly, when recorded at very low scan rates ($1\,mV\,s^{-1}$) under thin-layer conditions, the electrochemical behaviour of compound **1a** (Figure 5) becomes similar to that

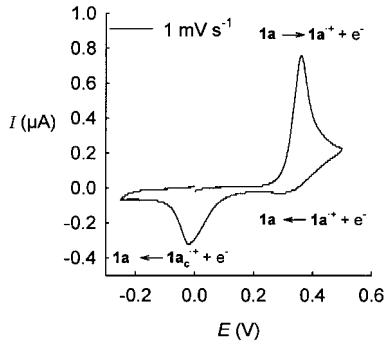

Figure 5. Experimental cyclic voltammogram in thin layer conditions ($d \approx 50\,\mu m$) for **1a** ($3.1\times10^{-3}\,mol\,L^{-1}$), at 293 K, in $5\times10^{-1}\,mol\,L^{-1}$ TBAHP/ACN/CH_2Cl_2; reference electrode Ag/AgCl.

observed for **1b** at $300\,V\,s^{-1}$. A voltammetry study versus scan rates, performed in semi-infinite diffusion conditions (Figure 6, top), validates this effect. Indeed, the electrochemical reversibility of the first oxidation step of compound **1a** is progressively altered upon decreasing the scan rate; this

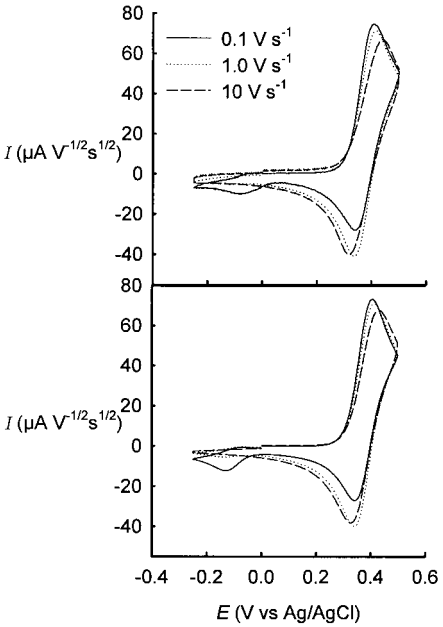

Figure 6. Experimental (top) and simulated (bottom) cyclic voltammograms of compound **1a**. The simulated data (DIGISIM 2.1®) were fitted to experimental results for **1a** ($3.1\times10^{-3}\,mol\,L^{-1}$ and $3.1\times10^{-4}\,mol\,L^{-1}$) at 293 K according to Scheme 6. All simulations were carried out with the same set of parameters, only the scan rate changed according to the experimental voltammograms. (10, 5, 2, 1, 0.5, 0.2 and $0.1\,V\,s^{-1}$). For clarity reasons, only three among seven scan rates are represented for $c=3.1\times10^{-3}\,mol\,L^{-1}$. Charge transfer parameters: $E=0.377$ V vs. Ag/AgCl, $E_c=-0.108$ V vs. Ag/AgCl, $k_s=0.1\,cm\,s^{-1}$, $\alpha=0.5$. Chemical reaction parameters: $K_0=10^8$, $k_{0f}=5\times10^4\,s^{-1}$ and $K_1=2.5$, $k_{1f}=3\times10^{-1}\,s^{-1}$. Diffusion coefficient: $D=3.1\times10^{-5}\,cm^2\,s^{-1}$.

phenomenon can be correlated to the appearance of a reduction peak for a negative potential value during the backward scan, as for **1b**. A quantitative analysis of the data over the scan-rate range investigated (Figure 6, bottom), based on Scheme 6 and performed in the same conditions as for **1b**, confirms that compounds **1a** and **1b** actually present the same electrochemical behaviour, but for shifted scan-rate windows.

The ratio of the kinetic constants obtained by fitted parameters for the forward reaction of compounds **1b** ($k_{1f}=2\times10^2\,s^{-1}$) and **1a** ($k_{1f}=3\times10^{-1}\,s^{-1}$) is close to 700, which explains the electrochemical irreversibility observed upon oxidation of **1b.** Thermodynamic equilibrium constants (K_1) confirm these conclusions, with a clear evidence of a stronger stabilization of the $\mathbf{1b_c}^{\bullet+}$ species ($K_1=4\times10^2$) related to $\mathbf{1a_c}^{\bullet+}$ ($K_1=2.5$) in their respective equilibria with the corresponding neutral donors.

The bis(2,6(7)-dithiafulvenyl)-TTF derivatives **4**–**6** were also studied by means of cyclic voltammetry (Table 1). Here again, the shape of the voltammograms is highly affected by the nature of the R substituent grafted on the peripheral dithiafulvenyl moieties. As for their monosubstituted analogues, compounds **4a**, **5a** and **6a**, which incorporate two dithiafulvenyl fragments substituted with carbomethoxy groups, exhibit two reversible redox systems under standard conditions ($100\,mV\,s^{-1}$). The oxidation potentials of **1a** and **4a** are roughly similar, which constitutes an additional evidence of the poor contribution of the lateral dithiafulvenyl rings, when substituted with $R=CO_2Me$, to the π-donating ability of the molecule. These oxidation potentials are shifted towards positive values when going from **4a** to **5a** and from **5a** to **6a**, in accordance with the withdrawing effect of the substituents directly grafted onto the electroactive TTF framework (**4a**: H; **5a**: CO_2Et; **6a**: CN).

The extended systems **4b**, **5c**, **5d** and **6c** display voltammograms somewhat more difficult to interpret, since they involve multiredox processes. Nevertheless, as in the case of its monosubstituted analogue **1b**, compound **4b**, which is substituted with electron-donating Me groups, exhibits a negative E^1_{red} value, leading to a $\Delta E=E^1_{ox}-E^1_{red}=0.44$ V, which confirms the precedent observations made on monosubstituted TTF derivatives.

X-ray crystal structure of 1a: Single crystals of **1a** were obtained from slow evaporation of a chloroform/cyclohexane solution. The molecular X-ray structure[23] of **1a** (Figure 7) shows the lateral dithiafulvenyl moiety to roughly extend along the long axis of the central TTF skeleton, in a conformation close to that of conformation A depicted in Figure 8, but with significant deviations from the molecular plane. Thus, contrary to vicinal bis-substituted dithiafulvenyl TTF systems of type **I**,[3] in which both outer S heterocycles adopt conformation B (Figure 8), there is clearly no 1,5-S···S intramolecular bonding interaction in **1a**. Moreover, the lack of planarity of the donor molecule constitutes an additional argument to explain the poor contribution of the adjacent dithiafulvenyl ring to the π-donating ability of the donor molecule.

 © WILEY-VCH Verlag GmbH, D-69451 Weinheim, 2000 0947-6539/00/0607-1204 $ 17.50+.50/0 *Chem. Eur. J.* **2000**, *6*, No. 7

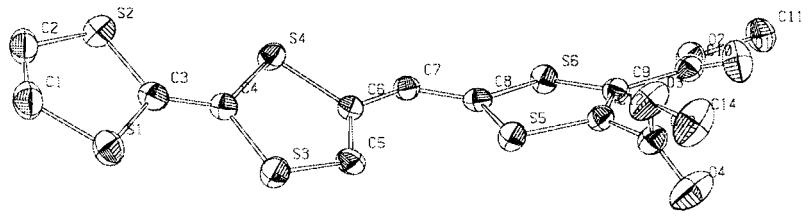

Figure 7. ORTEP view of **1a.**

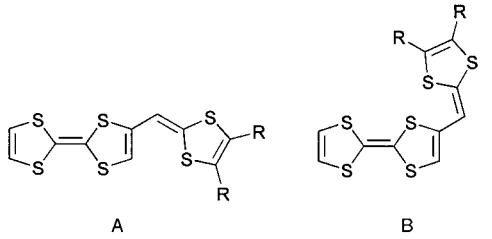

Figure 8. Conformations A and B expected for compounds **1**–**3**.

Theoretical calculations: The molecular structure and electronic properties of compounds **1a**, **1b** and **1d**, on both neutral and oxidised states, were theoretically investigated within the density functional theory (DFT) by using the B3P86 density functional and the 6–31G* polarised basis set. Compared to standard ab initio Hartree-Fock (HF) methods, DFT calculations have the advantage of including electron correlation effects and have been shown to provide molecular geometries in better agreement with X-ray structural data for extended TTFs.[24] For the unsubstituted compound **1d**, calculations were also performed at the more accurate MP2 (second-order Møller-Plesset perturbation theory) level to check the reliability of DFT results.

Neutral compounds: The molecular structures of **1a**, **1b** and **1d** were optimised by considering the two conformations depicted in Figure 8. Conformation A places the lateral dithiafulvenyl substituent along the long axis of the TTF skeleton as experimentally observed in the X-ray structure of **1a**. In conformation B the dithiafulvenyl moiety "faces" the TTF core and gives rise to an intramolecular 1,5-S···S interaction. This interaction is present in vicinal-disubstituted dithiafulvenyl TTFs like **I**[3] and in a variety of TTF analogues and derivatives.[22, 25] For compound **1d**, conformations A and B were optimised both assuming a C_s planar structure and without imposing any symmetry restriction.

B3P86/6–31G* calculations predict that conformation A is slightly more stable than conformation B by 0.36 (**1a**), 0.34 (**1b**) and 0.54 kcal mol^{-1} (**1d**). MP2/6–31G* calculations lead to the same conclusion for **1d** and increase the energy difference to 1.00 kcal mol^{-1}. These results agree with the X-ray structure observed for **1a** and show that the substituents attached to the external dithiafulvenyl ring only have a small influence on the relative stability of conformers A and B. The 1,5-S···S interaction that takes place in conformation B is usually invoked as a stabilising bonding interaction and is calculated to occur at an optimised distance of 3.19 Å independently of the substituent. Although this distance is significantly shorter than the sum of the van der Waals radii (3.60 Å),[26] it is slightly longer than the distance observed for systems like 2,5-bis(1,4-dithiafulven-6-yl)thiophene for which both dithiafulvenyl groups prefer to orientate in a B conformation and give rise to two simultaneous 1,5-S···S interactions at 3.12 Å.[25c] The main difference between this system and the compounds studied here is that for the former the 1,5-S···S interaction takes place between thiophene and 1,3-dithiole rings, while for the latter the interaction occurs between dithiole rings. This difference is the only apparent reason of the lower stability of conformation B for compounds **1**.

As depicted in Figure 9a, the minimum-energy conformation calculated for compounds **1** is distorted from planarity. For unsubstituted **1d**, this conformation is calculated to be more stable than the fully planar structure by 0.67 kcal mol^{-1} at the B3P86 level (2.42 kcal mol^{-1} at the MP2 level). The small energy gap that separates the folded structure from the

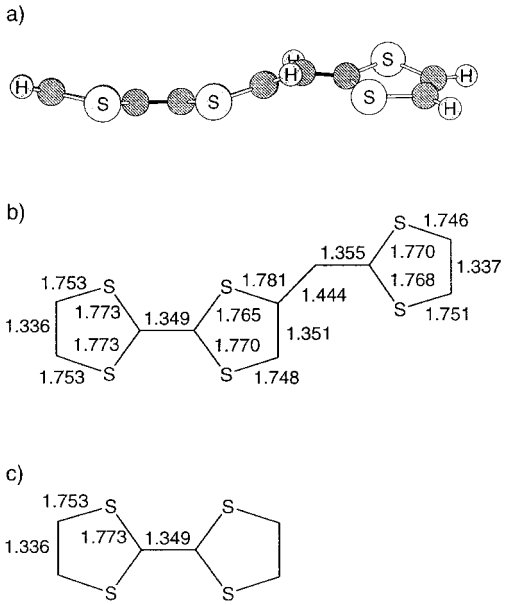

Figure 9. a) Minimum-energy conformation calculated for **1d**. Optimised bond lengths (in Å) for b) **1d** and c) TTF. All the structural data were obtained at the B3P86/6–31G* level.

planar form agrees with the high flexibility recently suggested both experimentally[27a] and theoretically[27b] for the TTF core. In going from left to right in Figure 9a, the dithiole rings are folded along the S···S axes by 13.7°, 18.6° and 7.0° (17.3°, 24.0° and 11.7° at the MP2 level). These values slightly change in passing to **1a** (13.7°, 14.6° and 12.5°) and **1b** (14.0°, 14.1° and 7.1°) and overestimate the average values obtained for **1a** from X-ray data (4.9°, 8.4° and 12.5°), since crystal packing tend to planarise the molecule. Moreover, the dithiafulvenyl substituent is rotated around the C6–C7 single bond, partially breaking the conjugation with the TTF core. The rotational angle C5-C6-C7-C8 calculated at the B3P86 level is 28.2° for **1a**, 20.9° for **1b** and 25.7° (35.2° at the MP2 level) for

1d in good agreement with the X-ray value observed for **1a** (28.2°).

The average deviations between the X-ray data and the theoretical parameters calculated for **1a** are 0.017 Å for the bond lengths and 0.9° for the bond angles, showing the agreement between theory and experiment. Figure 9b indicates the optimised bond lengths computed for the minimum-energy conformation of **1d** at the B3P86 level. The geometries of the three dithiole rings are very similar and their bond lengths closely correspond to those of parent TTF (cf. Figure 9b and 9c). It is, however, important to note the asymmetry observed for the central dithiole ring, for which the S4–C6 and S3–C5 bonds have lengths of 1.781 and 1.748 Å, respectively. These slightly different values indicate some degree of conjugation of the dithiafulvenyl ring with the TTF core through the C6–C5 and C5–S3 bonds, which are respectively longer and shorter than in TTF. This trend is confirmed at the MP2 level for **1d** and is also found for **1a** and **1b**.

Figure 10 shows the atomic orbital (AO) composition of the highest occupied molecular orbital (HOMO) of **1d**. Similar topologies are found for **1a** and **1b**. The fact that the HOMO resides mostly on the TTF moiety suggests that the first

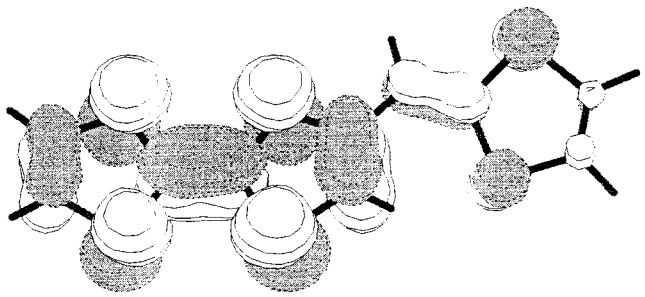

Figure 10. Electronic density contours calculated for the HOMO of **1d** at the B3P86/6–31G* level.

electron in the oxidation process is extracted mainly from the TTF backbone and that the substituents of the dithiafulvenyl group should not affect the first oxidation potential. None of these suggestions is completely true. On the one hand, the external dithiole ring actively participates in the oxidation process as discussed below. On the other hand, the energy of the HOMO depends on the electron-attracting or electron-releasing character of the substituent and increases along the series: **1a** (−5.16 eV), **1d** (−5.08 eV), **1b** (−5.00 eV). Since less positive oxidation potentials are to be expected for compounds with higher energy HOMOs, this trend justifies the cathodic shift of 0.18 V experimentally observed in passing from to **1a** to **1b** (see Table 1).

Oxidised compounds: To get a deeper understanding of the oxidation process, the molecular geometries of the radical cation and dication of **1a**, **1b** and **1d** were optimised at the B3P86/6–31G* level. In contrast with that obtained for the neutral molecules, conformation B is calculated to be more stable for both the cation and the dication. For the cation, the energy differences between the fully optimised conformations A and B are 1.03 (**1a**), 1.28 (**1b**) and 1.07 kcal mol^{-1} (**1d**). For the dication, these energies increase to 3.51, 3.45 and 3.11 kcal mol^{-1}, respectively. The dication of **1d** was also calculated at the MP2 level and an energy difference of 4.06 kcal mol^{-1} was obtained.[28] Besides the modification of the conformational preferences of the molecule, the oxidation process induces the planarisation of the molecular structure for both the cation and dication. The maximum deviations from planarity are of 0.4° for the folding of the dithiole rings and 2.2° for the rotation around the C6–C7 bond of the external dithiafulvenyl group.

The bond lengths calculated for $\mathbf{1d}^{\bullet+}$ and $\mathbf{1d}^{2+}$ are displayed in Figure 11 to be compared with those given in Figure 9b for neutral **1d**. They clearly show that the oxidation process affects both the TTF moiety and the dithiafulvenyl group. For both the cation and the dication, the outer dithiole rings are structurally identical, their bond lengths differing by less than 0.005 Å. In passing to the dication, the S–C bonds shorten to 1.72–1.73 Å and the C=C bonds lengthen to 1.350 Å. Relative to the parent TTF, these lengths are intermediate between those of the radical cation (Figure 11c) and those of the dication (Figure 11d); this suggests that each of the outer rings in $\mathbf{1d}^{2+}$ holds a positive charge between 0.5 and 1.0 e.

The central dithiole ring in $\mathbf{1d}^{\bullet+}$ and $\mathbf{1d}^{2+}$ presents a completely different structure and is highly asymmetric. In passing from **1d** to the dication, the S3–C4 and S3–C5 bond

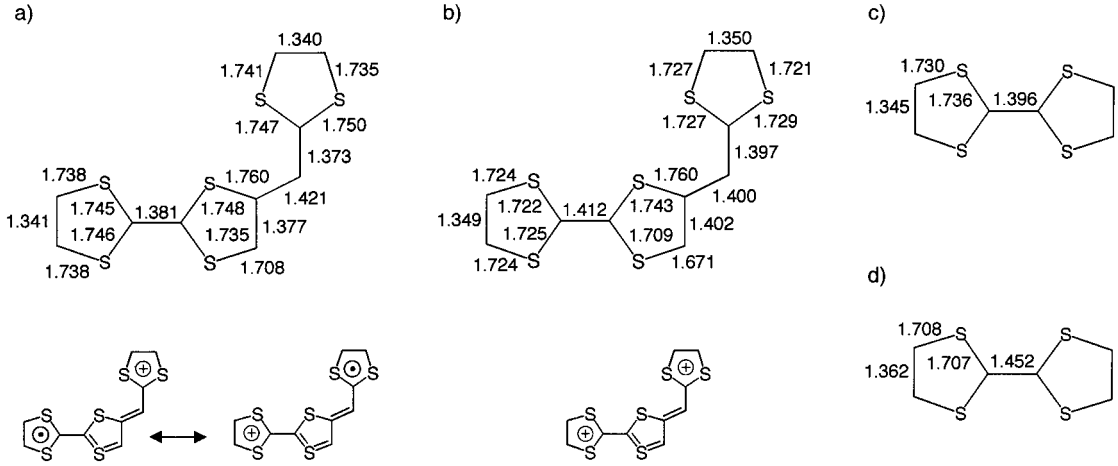

Figure 11. B3P86/6–31G*-optimised bond lengths (in Å) for a) $\mathbf{1d}^{\bullet+}$, b) $\mathbf{1d}^{2+}$, c) $TTF^{\bullet+}$ and d) TTF^{2+}. Resonance structures are included for $\mathbf{1d}^{\bullet+}$ and $\mathbf{1d}^{2+}$.

© WILEY-VCH Verlag GmbH, D-69451 Weinheim, 2000
0947-6539/00/0607-1206 $ 17.50+.50/0 *Chem. Eur. J.* **2000**, *6*, No. 7

lengths reduce drastically from 1.770 to 1.709 Å and from 1.748 to 1.671 Å, respectively. In contrast, the S4–C4 and S4–C6 bonds are only slightly shortened from 1.765 to 1.743 Å and from 1.781 to 1.760 Å, respectively. It is also worth noting that the C5–C6, C6–C7 and C7–C8 bond lengths are equal upon oxidation (cf. Figures 9b, 11a and 11b). The values obtained for $\mathbf{1d}^{2+}$ (1.402, 1.400 and 1.397 Å, respectively) are typical of fully delocalised C_{sp^2}–C_{sp^2} bonds as in benzene (1.40 Å). These structural trends are confirmed at the MP2 level and indicate that a conjugation path is established between the outer dithiole rings through the lower part of the central ring (i.e., through the S3–C4, S3–C5 and C5–C6 bonds), in which the S4–C4 and S4–C6 bonds do not participate. The bond lengths calculated for S3–C4 and S3–C5 in the dication are in fact intermediate between those computed for thiophene (1.724 Å)[29] and that of a purely localised C=S double bond as in $H_2C{=}S{=}CH_2$ (1.642 Å).[30] This suggests that resonance forms involving tetravalent sulfur, such as those depicted in Figures 11a and 11b (bottom), contribute to the molecular structure of the radical cation and dication of **1d**. This type of resonance structure has been invoked by different authors to explain the higher aromaticity of thiophene and related compounds when compared with furan and pyrrole derivatives,[31] and has been intensively investigated for the thieno[3,4-c]thiophene series.[30, 32]

The Mulliken net atomic-charge distributions calculated for **1d**, $\mathbf{1d}^{\bullet+}$ and $\mathbf{1d}^{2+}$ (Table 2) support the structural trends discussed above. On the one hand, electrons are removed in a similar proportion from the three dithiole rings, thus supporting the participation of the three rings in the oxidation process. For the radical cation, 0.37 e are taken from the unsubstituted ring of TTF, 0.32 e from the central ring and 0.31 e from the dithiafulvenyl group. For the dication, the charges extracted increase to 0.72, 0.60 and 0.68 e, respectively. On the other hand, the extra charge is distributed in a different way in the three dithiole rings. For the outer rings, it is almost equally shared by both sulphur environments. For the central ring, the extra charge is mainly accumulated on the S3-C5-H5 atoms, from which 0.45 e are removed in $\mathbf{1d}^{\bullet+}$, thus showing the asymmetry of this ring.

Table 2. B3P86/6–31G* net atomic charges [e] calculated for **1d** and its radical cation and dication by using Mulliken population analysis.

atom[a]	**1d**[b]	$\mathbf{1d}^{\bullet+}$[c]	$\mathbf{1d}^{2+}$[c]
C1	−0.33	−0.33	−0.32
H1	0.22	0.27	0.32
C2	−0.33	−0.33	−0.33
H2	0.22	0.27	0.32
S1	0.28	0.42	0.54
S2	0.28	0.41	0.53
C3	−0.34	−0.34	−0.34
C4	−0.33	−0.37	−0.39
S3	0.28	0.45	0.60
S4	0.27	0.42	0.49
C5	−0.39	−0.39	−0.35
H5	0.23	0.26	0.32
C6	−0.09	−0.10	−0.12
C7	−0.20	−0.17	−0.15
H7	0.19	0.22	0.26
C8	−0.32	−0.35	−0.36
S5	0.30	0.40	0.49
S6	0.29	0.40	0.53
C9	−0.33	−0.33	−0.32
H9	0.22	0.27	0.31
C12	−0.34	−0.35	−0.34
H12	0.22	0.26	0.31

[a] See Figure 7 for atom numbering. [b] A conformation. [c] B conformation.

Identical structural trends to those discussed above for unsubstituted **1d** are obtained for **1a** and **1b** upon oxidation. The bond lengths calculated for the radical cations and dications of **1a** and **1b** differ by less than 0.001 Å from those given in Figure 11 for $\mathbf{1d}^{\bullet+}$ and $\mathbf{1d}^{2+}$. Substituents only have a small effect on the adjacent S6–C9, S5–C12 and C9–C12 bonds, which lengthen by 0.01 Å for both $\mathbf{1a}^{2+}$ and $\mathbf{1b}^{2+}$. As for **1d**, electrons are removed from the whole molecule and the charges extracted from each dithiole environment have similar values ($\mathbf{1a}^{2+}$: 0.71, 0.57 and 0.72 e; $\mathbf{1b}^{2+}$: 0.67, 0.53 and 0.80 e).

The evolution upon oxidation of the molecular structure and the distribution of the extra charge found for compounds **1** thus suggest that these extended TTF derivatives should not be visualised as conventional substituted TTFs. Theoretical results show that the central dithiole moiety actually acts as a conjugate spacer between the outer dithiole rings. The conjugation path is established through the C3=C4-S3-C5=C6-C7=C8 chain, which, in principle, does not offer a fully conjugated pathway in contrast to the polyene spacers present in TTF vinylogues.

We believe that these particular structural features are the reason for the unconventional electrochemical behaviour presented by the TTF derivatives synthesised here whatever the electronic character of their substituents (**a**, **b** and **d** series) is. Upon oxidation, the external dithiole rings are aromatised and the conjugation path becomes fully delocalised with C–C bonds of 1.40 Å and rather short S–C bonds, which involve partial tetravalent character for S3. Once the molecule is oxidised and the dication obtained, the reduction of the dication to the radical cation is reversible because the molecular structure remains highly delocalised (see resonance forms in Figure 11). Therefore, this highly delocalized radical cation may correspond to the peculiar stabilised structure considered in the electrochemical part, denoted as $\mathbf{1b}_{\mathbf{c}}^{\bullet+}$ (in the case of donor **1b**). In contrast, when passing from the radical cation to the neutral molecule, the structure loses the stability provided by the tetravalent resonance forms and, as a consequence, the effective conjugation between the external rings; it therefore becomes a substituted TTF, that is, a less conjugated system. This loss of conjugation could explain the cathodic shift of the reduction of the cation, thus determining the electrochemical irreversibility of the first oxidation wave.

In order to learn more about the relationship between the chemical structure of these extended TTFs and their electrochemical behaviour, the molecular structure of the bis(dithiafulvenyl)-TTF derivative **III**[3] was investigated at the B3P86/6–31G* level (see Figure 12). The neutral molecule is slightly distorted from planarity with the dithiafulvenyl groups twisted by 21° and shows approximately C_2 symmetry. The dication is fully planar and has C_{2v} symmetry; it exhibits two short 1,5-S···S contacts at 3.07 Å. The bond lengths displayed in Figure 12 (middle) for **III** are typical of a neutral TTF and

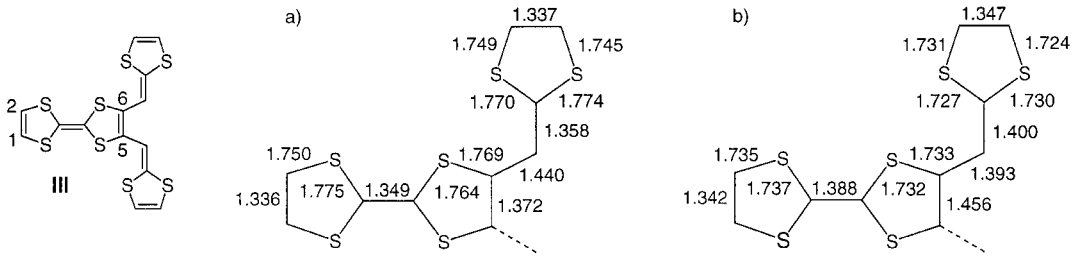

Figure 12. B3P86/6–31G*-optimised bond lengths (in Å) for a) **III** (C_2 symmetry) and b) **III**$^{2+}$ (C_{2v} symmetry).

are similar to those given in Figure 9b for **1d**. It is however to be noted that the C5–C6 bond (1.372 Å) is 0.04 Å longer than the C1–C2 bond, which has a length identical to that calculated for neutral TTF (1.336 Å). The length of the C5–C6 bond suggests that a conjugation path is established between the two dithiafulvenyl groups through the C5–C6 bond. This suggestion is confirmed by the geometry obtained for **III**$^{2+}$, for which the C5–C6 bond lengthens to 1.456 Å, while the equivalent C1–C2 bond on the other side of TTF remains almost unaffected. Molecule **III** actually behaves as a mixed system with properties resulting from the TTF vinylogue formed by the two dithiafulvenyl substituents and the C5–C6 bond and from the TTF backbone. On going from **III** to **III**$^{2+}$, 1.16 e are extracted from the dithiafulvenyl groups and 0.84 e from the TTF backbone, in accord with the well-known fact that TTFs vinylogues are slightly better donors than TTF itself.[33] These structural and electronic features justify the electrochemical properties of **III**, for which two reversible redox processes, almost coalesced in most solvents, are found at potentials slightly lower than in TTF.[3]

The results obtained for **III** indicate a clear difference between this vicinal-disubstituted system and the monosubstituted compounds **1**. For **III**, the TTF backbone acts as a bridge between the dithiafulvenyl substituents forming a TTF vinylogue and preserves, at the same time, the structure and properties of the TTF core. For **1**, the TTF backbone loses its identity upon oxidation, since a special connection is established between the dithiafulvenyl substituent and the TTF ring opposite to it. These structural differences determine the completely different electrochemical behaviour found for **III** and **1**.

It should be mentioned that both neutral and oxidised states of compound **4d** were also calculated, as an example of a bis(dithiafulvenyl)-TTF for which substitution is performed on both dithiole rings of TTF. Compound **4d** behaves similarly to compounds **1**. For the dication, a conjugation path involving two sulfur atoms with partial tetravalent character is established between the external dithiafulvenyl groups. The whole TTF core now acts as a spacer and the existence of two equivalent dithiafulvenyl moieties facilitates the extraction of two electrons at similar oxidation potentials (see Table 1).

Solvent effects: The theoretical calculations discussed until now give no argument to justify the different electrochemical behaviour found for compounds bearing electron-attracting carbomethoxy groups (**a**) or electron-releasing methyl groups (**b**). The structural (preferred conformation, evolution of the molecular structure upon oxidation) and electronic (charge distribution) trends are the same for **1a** and **1b** and for unsubstituted **1d**; this suggests that the nature of the substituents attached to the dithiafulvenyl groups has a negligible effect. It should, however, be pointed out that calculations were performed for isolated molecules (in vacuum) and that the electrochemical properties are measured in solution. To investigate the influence of the solvent, the molecular structures of **1a** and **1b** were recalculated at the PM3 semiempirical level by using the COSMO model for the solvent. Prior to these calculations, the applicability of the PM3 approach was tested by optimising the molecular structures of neutral and oxidised **1a** and **1b** in vacuum. The geometries provided by the PM3 method are very similar to those obtained at the B3P86/6–31G* level and reproduce all the structural trends discussed above.

The solvent has no relevant effect on the molecular and electronic structures of the neutral compounds, but drastically affects the charged species. As shown in Figure 13, the minimum-energy conformation calculated for **1a**$^{2+}$ in CH_2Cl_2 (dielectric constant $\varepsilon = 9.08$) is non-planar due to the rotation of the TTF rings around the C3–C4 bond. The optimised bond lengths clearly show that the molecular structure of **1a**$^{2+}$ corresponds to a doubly charged TTF core substituted with

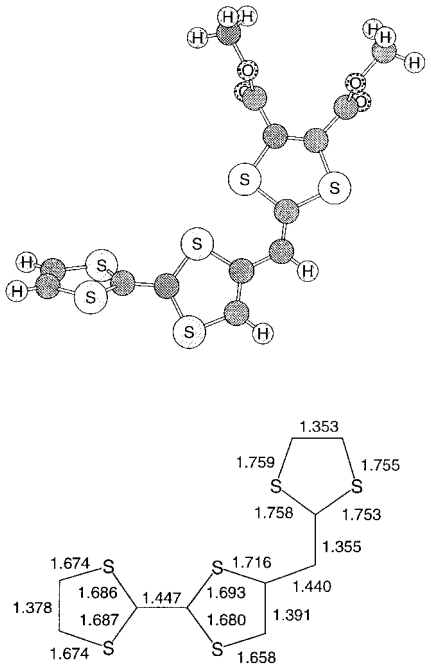

Figure 13. Minimun-energy conformation and optimised bond lengths (in Å) calculated for **1a**$^{2+}$ in solution (CH_2Cl_2) at the PM3 level.

 © WILEY-VCH Verlag GmbH, D-69451 Weinheim, 2000 0947-6539/00/0607-1208 $ 17.50+.50/0 *Chem. Eur. J.* **2000**, *6*, No. 7

a neutral dithiafulvenyl ring. This picture is supported by the net atomic-charge distribution, since a total of 1.85 e are extracted from the TTF core, with the remaining 0.15 e being removed from the dithiafulvenyl moiety.

The solvent therefore favours the localisation of the extra charge on the TTF core. This is in contrast with the delocalised structure found in vacuum, in which charge is extracted almost equally from the three dithiole moieties. The stabilisation of the localised structure versus the delocalised one can be understood as resulting from the interaction of the molecular dipole moment with the solvent. For $\mathbf{1a}^{2+}$, the dipole moment increases from an already high value of 16.9 D for the delocalised structure found in vacuum to a very large value of 35.4 D for the localised structure calculated in the solvent. The huge increase of the dipole moment is due to the accumulation of the positive charge on the TTF backbone.

Theoretical calculations therefore suggest that, in the presence of the solvent, electrons are removed from the TTF core and compound **1a** behaves as a substituted TTF. This result explains the experimental finding that **1a** has two reversible oxidation processes at nearly the same potential values as TTF. The third oxidation process observed at 1.6 V then corresponds to the oxidation of the dithiafulvenyl ring.

PM3 calculations predict the same behaviour for the methyl-substituted compound **1b** in CH_2Cl_2. Though compounds **1a** and **1b** follow the same electrochemical square scheme, kinetic and thermodynamic constants involved in Scheme 6 are clearly distinct between the two families, as shown by electrochemical experiments. There are, however, some reasons to support the idea that solvent effects are more intense for the cations of **1a** than for the cations of **1b**. On the one hand, **1b** is a less polar molecule. The dipole moment of $\mathbf{1b}^{2+}$ increases from 3.2 D (delocalised form in vacuum) to 21.0 D (localised form in CH_2Cl_2) compared with the values of 16.9 and 35.4 D found for $\mathbf{1a}^{2+}$. On the other hand, the localised structure is perfectly preserved in $\mathbf{1a}^{2+}$ for values of the dielectric constant as low as 2.0. This is not the case for $\mathbf{1b}^{2+}$, for which the localised structure evolves to the delocalised one as the dielectric constant diminishes and a fully planar delocalised structure identical to that found in vacuum is obtained for low values of ε. This means that localised structures with the charge accumulated on the TTF core are energetically less favoured for **1b** than for **1a** owing to solvent effects or, in other words, that delocalised structures are more easily achieved for the cations of **1b**. If, as suggested above, the $\mathbf{1b}_c^{\bullet+}$ species used in Scheme 6 is identified with the delocalised structure, the theoretical results then support the higher values obtained for the k_{1f} and K_1 constants of **1b** relative to **1a**, since these constants would imply the formation of delocalised forms that are more readily accessible for **1b** than for **1a**.

It can be therefore concluded that substituents in compounds **1** play an important role in the electrochemical properties owing to the interactions with the solvent. Carbomethoxy groups give rise to more polar cations than methyl-substituted compounds and form localised structures in which the charge accumulates on the TTF core more easily. The stabilisation of these structures determines an electrochemical behavior similar to TTF.

It should be mentioned that more elaborated solvent models and more accurate quantum-chemistry methods would be required to provide a quantitative description of the influence of the solvent that allows theoretical calculations to make an unambiguous distinction between carbomethoxy- and methyl-substituted derivatives. The size and asymmetry of the molecules studied in this work makes it especially difficult to perform a more precise study.

Nonlinear optical properties: The structural originality of compounds **5** and **6** lies in the coexistence of electron-donating (dithiafulvenyl) and electron-withdrawing (carbomethoxy or cyano) substituents on the electroactive TTF framework. This association provides multiple potential donor–acceptor conjugation paths through the TTF core, and should fulfill requisite criteria to reach active third-order nonlinear optical structures.[16a]

Third-order susceptibilities χ^3 of compounds **5** and **6** were measured[34] by the degenerate four-wave mixing method. The excitation is provided by 30 ps light pulses at 532 nm. Compounds **5** and **6** reveal large second-order nonlinear optical hyperpolarisability γ, the best result being obtained for **5a** with a value of $\gamma^{\text{electronic}}$ 24×10^4 times greater than that for CS_2; this constitutes an important improvement relative to other conjugated TTF derivatives studied so far.[35]

Considering these promising results attempts of grafting other electron-donating and electron-withdrawing substituents onto the TTF core are in progress in order to establish the relationship between the hyperpolarisability γ and the most significant structural and electronic parameters.

Conclusion

Novel, highly extended TTF derivatives bearing electron-donating groups (as well as electron-withdrawing groups in some cases) have been prepared thanks to various synthetic methodologies. The electrochemical study of these compounds (**1**–**6**) reveals that the shape of the voltammogram strongly depends on the nature of the R substitution. Compounds of the **a** series, which incorporate dithiafulvenyl moieties substituted with electron-withdrawing carbomethoxy groups, present an electrochemical behaviour typical of a TTF derivative with two reversible one-electron redox systems below 1.00 V. Surprisingly, a new reduction wave corresponding to the radical-cation/neutral donor redox process appears for very low scan rates. In the case of compounds of the **b** ($R = CH_3$) and **d** ($R = H$) series, the same unusual electrochemical behaviour is observed, but under standard CV conditions (i.e., scan rate: 100 mV s^{-1}). Digital simulation of the electrochemical data has allowed the description of the square scheme involved on cycling. These unusual electrochemical properties have been investigated by means of theoretical calculations in order to get structural insights about the oxidised species generated. In the gas phase, no relevant difference is detected as a function of the substitution patterns. Neutral molecules are predicted to be in an A conformation (Figure 8), which is slightly distorted from planarity and in accord with X-ray crystal structure data. The

oxidised compounds (cations and dications) prefer to adopt a B conformation (Figure 8) and delocalise the extra charge over the whole molecule. The resulting structures do not correspond to an oxidised TTF and are stabilised by resonant forms that involve tetravalent sulphur atoms, which form part of the fully delocalised pathway established between the outer dithiole moieties. These structural features explain the unconventional electrochemical properties observed for those derivatives. When effects of the solvent are taken into account, calculations predict localised structures for oxidised compounds, in which the charge is extracted from the TTF backbone and the dithiafulvenyl rings remain neutral. These localised structures are more easily obtained for compounds of the **a** series owing to their higher polarity and justify the fact that they electrochemically behave as substituted TTFs under standard CV conditions.

Experimental Section

Melting points were obtained from a Rechert-Jung hot-stage microscope apparatus and are uncorrected. IR spectra were recorded on a Perkin–Elmer model 841 spectrophotometer, samples being either nujol mulls, embedded in KBr discs, or thin films between NaCl plates. ^{1}H NMR and ^{13}C NMR spectra were recorded on a Jeol GSX270WB spectrometer, operating at 270 and 67.5 MHz, respectively; δ are given in ppm (relative to TMS) and coupling constants (J) in Hz. Mass spectra were recorded under EI or FAB mode on a VG Autospec mass spectrometer. UV/Vis spectra were recorded on a Perkin–Elmer Lambda 2 spectrometer. Elemental analyses were performed by the Service central d'analyses du CNRS (Vernaison, France). Column chromatography separations and purifications were carried out on Merck silica-gel 60 (0.040–0.0063 nm).

Electrochemistry: Cyclic voltammetric experiments have been carried out at $20 \pm 0.1\,^{\circ}$C with an EGG PAR 273 electrochemical analyzer, in a three-electrode cell (SCE or Ag/AgCl reference). The working electrode was a platinum disk (2 mm diameter) polished to a mirror finish. Platinum wires were used as auxiliary and pseudo-reference electrodes. An ohmic drop compensation was applied when necessary. The experimental setup for the spectroelectrochemistry experiments has been previously described.[36] The cell used can be operated either under semi-infinite diffusion or thin-layer conditions.

X-ray diffraction: Data collection was carried out on an Enraf-Nonius CAD4 diffractometer.[23] Crystallographic data (excluding structure factors) for the structures reported in this paper have been deposited with the Cambridge Crystallographic Data Centre as supplementary publication no. CCDC-128517. Copies of the data can be obtained free of charge on application to CCDC, 12 Union Road, Cambridge CB2 1EZ, UK (fax: (+44) 1223-336-033; e-mail: deposit@ccdc.cam.ac.uk).

Computational methods: Calculations were performed on IBM RS/6000 workstations and on a SGI-ORIGIN 2000 computer at the Departamento de Química Física of the University of Valencia. Geometry optimisations were carried out at the density functional theory (DFT) level using the hybrid, gradient-corrected B3P86 density functional[37] and the split-valence, double-ζ, polarised 6–31G* basis set.[38] Additional optimisations were done at the second-order Møller-Plesset (MP2) perturbation theory level with the same basis set. The geometries of neutral molecules and dications were computed within the restricted Hartree–Fock (RHF) formalism, while the spin-unrestricted Hartree–Fock (UHF)[39] approximation, in which electrons with different spins occupy different sets of orbitals, was used for singly charged cations. The Berny analytical method[40] was employed for the optimisations, and the threshold values for the maximum force and the maximum displacement were 0.00045 and 0.0018 au, respectively. All DFT and MP2 calculations were performed with the Gaussian 94 suite of programs.[41] Geometry optimisations including solvent effects were carried out at the PM3 semiempirical level[42] using the conductor-like screening model (COSMO) approach[43] as implemented in the MOPAC93 package program.[44] The COSMO model, as other continuum models,[45] assimilates the solvent to a continuos medium characterised by a dielectric constant ε and which surrounds a molecular-shaped cavity in which the solute is placed. It generates a conducting polygonal surface around the molecule at the van der Waal's distance and replaces the dielectric outside the cavity with a conductor.

Wittig mono- and diolefinations

General procedure: Wittig polyolefinations were achieved by reaction between (poly)formyl compounds **7**–**12** and phosphorous ylides **Wa**–**d**. Ylides **Wb**–**d** were generated at low temperature with *n*BuLi as a base, from the corresponding phosphonium salts, which were prepared in situ by interaction between equimolar amounts of triphenylphoshine and the corresponding 1,3-dithiolium salts[7] (*method A*). In the case of R = CO_2Me, **Wa** was prepared according to the literature[6] (*method B*), except for the synthesis of **3a** (see below).

Method A (R = CH_3, SCH_3, H): The appropriate R-substituted phosphonium salt[7] was generated in dry acetonitrile under nitrogen. After 15 min of stirring at RT, the reaction mixture was diluted with dry THF, cooled to $-75\,^{\circ}$C and finally treated dropwise with 1 equivalent of *n*-butyl-lithium (1.6 M in *n*-hexane). The yellow solution of **Wb**–**d** was stirred for 10 min, and 0.91 equivalents of the monoformyl TTF derivative **7**–**9** or 0.45 equivalents of the diformyl TTF derivative **11** or **12** (a different method was used with compound **10**, see below) diluted in dry THF were introduced dropwise; the temperature was kept at $-75\,^{\circ}$C. At this stage, the colour of the solution invariably turned deep red. The reaction mixture was then allowed to warm to RT over a three hour period and was concentrated in vacuo. The crude material thus obtained was treated with methanol to allow precipitation of the olefination product. This was filtered on a sintered glass funnel and was thoroughly washed with hot methanol, acetonitrile and diethyl ether. Depending on their respective solubility and stability, the dark-red powders or microcrystals were recrystallised (see solvents hereafter) or purified by chromatography over silicagel.

Method B (R = CO_2Me): A solution of (4,5-dicarbomethoxy-1,3-dithiolyl)-tributylphosphonium tetrafluoroborate[6] and a formyl TTF derivative **7**–**12** (0.91 and 0.45 equivalents for single and twofold Wittig olefinations, respectively) in dry THF was stirred at RT under nitrogen. This solution was treated dropwise with a large excess of triethylamine and immmediately turned dark red. The reaction mixture was stirred at RT for 3 h and was concentrated in vacuo. Precipitation of the olefinated compound occured during the reaction or by adding methanol. The crude product was then filtered and thoroughly washed with various solvents or purified either by recrystallisation or silicagel chromatography, depending on its own stability and solubility.

2-(2,3-Bis(methoxycarbonyl)-1,4-dithiafulven-6-yl)-TTF (1a): Compound **1a** (method B) was synthesised by mixing the formyl-TTF **7** (232 mg, 1 mmol) and (4,5-dicarbomethoxy-1,3-dithiolyl)tributylphosphonium tetrafluoroborate[6] (1.1 equivalents) in dry THF (15 mL) and triethylamine (1 mL). After subsequent work-up, the crude product was recrystallised from toluene/petroleum ether to produce bright orange needles (280 mg, 65%). M.p. 161–62 °C; UV/Vis (CH_2Cl_2): $\lambda_{max} = 411$ nm; ^{1}H NMR (C_6D_6): $\delta = 5.37$ (s, 2H), 5.32 (s, 1H), 5.28 (s, 1H), 3.25 (s, 3H), 3.18 (s, 3H); MS (EI): m/z (%): 434 (100) $[M]^+$; elemental analysis calcd (%) for $C_{14}H_{10}O_4S_6$: C 38.69, H 2.32, O 14.72, S 44.27; found C 38.95, H 2.31, O 14.64, S 44.04.

2-(2,3-Dimethyl-1,4-dithiafulven-6-yl)-TTF (1b): Compound **1b**[20] (method A) was synthesised by starting from the formyl-TTF **7** (232 mg, 1 mmol). After subsequent work-up, it was recrystallised from dichloromethane/petroleum ether to produce dark orange crystals (210 mg, 61%). M.p. 173–75 °C; UV/Vis (CH_2Cl_2): $\lambda_{max} = 413$ nm; ^{1}H NMR ($CDCl_3$): $\delta = 6.31$ (s, 2H), 5.98 (s, 1H), 5.89 (s, 1H), 1.96 (s, 3H), 1.93 (s, 3H); MS (EI): m/z (%): 346 (75) $[M]^+$; elemental analysis calcd (%) for $C_{12}H_{10}S_6$: C 41.58, H 2.91, S 55.51; found C 41.50, H 2.91, S 55.44.

2-(2,3-Bis(methoxycarbonyl)-1,4-dithiafulven-6-yl)-6(7)-hydroxymethyl-TTF (2a): Compound **2a** (method B) was synthesised by mixing the TTF derivative **9** (100 mg, 0.38 mmol) and (4,5-dicarbomethoxy-1,3-dithiolyl)-tributylphosphonium tetrafluoroborate (1.1 equivalents) in dry THF (15 mL) and triethylamine (0.3 mL). After subsequent work-up, the crude product was purified by silicagel column chromatography (ethyl acetate/hexane, 1:1) and recrystallised from ethyl acetate/pentane, to afford **2a** as a brownish powder (130 mg, 74%). M.p. 142 °C; IR: $\tilde{\nu}_{max} = 1726$ cm^{-1} (C=O); ^{1}H NMR ([D$_6$]DMSO): $\delta = 6.55$ (s, 1H), 6.58 (s, 1H); 6.50 (s, 1H); 5.51 (br s, 1H), 4.20 (s, 2H); 3.77 (s, 6H); ^{13}C NMR ([D$_6$]DMSO): $\delta = 159.48$,

© WILEY-VCH Verlag GmbH, D-69451 Weinheim, 2000
0947-6539/00/0607-1210 $ 17.50+.50/0 *Chem. Eur. J.* **2000**, *6*, No. 7

158.96, 138.51, 131.72, 131.11, 130.72, 128.67, 117.65, 114.39, 111.75, 108.19, 107.39, 58.92, 53.80, 53.70; MS (EI): *m/z* (%): 464 (100) $[M]^+$; MS (HRMS, EI): *m/z*: 463.9000; $C_{15}H_{12}O_5S_6$ calcd 463.9009.

2-(2,3-Bis(methoxycarbonyl)-1,4-dithiafulven-6-yl)-6,7-(ethane-1,2-diyldisulfanyl)-TTF (3a):[46] Dry THF (25 mL) was added to a solution of (4,5-dicarbomethoxy-1,3-dithiolyl)tributylphosphonium tetrafluoroborate (140 mg, 0.275 mmol) in dry acetonitrile (8 mL), and the mixture was cooled at −80 °C under nitrogen. *n*BuLi (1.6 M in hexanes, 0.21 mL, 0.33 mmol) was added followed by a solution of compound **8** (80.5 mg, 0.25 mmol) in dry THF (15 mL) which was added dropwise. The reaction mixture was then allowed to warm to room temperature and was concentrated in vacuo. The crude reaction mixture was purified by silicagel column chromatography (methylene chloride/petroleum ether 1:1), to produce **3a** as a dark brown powder (53 mg, 40%). M.p. 138–142 °C; ^{1}H NMR ($CDCl_3$): $\delta = 6.03$ (s, 1H), 6.02 (s, 1H), 3.86 (s, 3H), 3.85 (s, 3H), 3.30 (s, 4H); MS (EI): *m/z* (%): 524 (45) $[M]^+$; MS (HRMS, EI): *m/z*: 523.8494; $C_{16}H_{12}O_4S_8$ calcd 523.8501.

2-(2,3-Dimethyl-1,4-dithiafulven-6-yl)-6,7-(ethane-1,2-diyldisulfanyl)-TTF (3b): Compound **3b** (method A) was synthesised by starting from the formyl-ethylenedithio-TTF **8** (80.5 mg, 0.25 mmol). The precipitate formed during the olefination reaction was filtered and thoroughly washed with methanol, acetonitrile and diethyl ether to afford **3b** as a brown powder (65 mg, 60%). M.p. 164 °C; ^{1}H NMR ($CDCl_3$): $\delta = 5.98$ (s, 1H), 5.89 (s, 1H), 3.29 (s, 4H), 1.96 (s, 3H), 1.93 (s, 3H); MS (EI): *m/z* (%): 436 (35) $[M]^+$; MS (HRMS, EI): *m/z*: 435.8697; $C_{14}H_{12}S_8$ calcd 435.8705.

2-(1,4-Dithiafulven-6-yl)-6,7-(ethane-1,2-diyldisulfanyl)-TTF (3d): Compound **3d** (method A) was synthesised by starting from the formyl-EDT-TTF **8** (150 mg, 0.47 mmol). The precipitate formed during the olefination reaction was filtered and thoroughly washed with methanol, acetonitrile and diethyl ether to afford **3d** as a brown powder (124 mg, 65%). M.p. 190 °C (decomp); ^{1}H NMR (CS_2/DCl_3 10:1): $\delta = 6.37$ (dd, $J = 6.6$, 0.5 Hz, 1H; SCH=C*H*S), 6.33 (dd, $J = 6.6$, 1.4 Hz, 1H; SC*H*=CHS), 6.04 (m, 1H; S_2C=CH), 5.92 (d, $J = 0.9$ Hz, 1H; SC*H*=C(S)CH), 3.32 (s, 4H); MS (EI): *m/z* (%): 408 (60) $[M]^+$.

2,6(7)-Bis(2,3-bis(methoxycarbonyl)-1,4-dithiafulven-6-yl)-TTF (4a): Compound **4a** (method B) was synthesised by mixing the TTF derivative **10** (100 mg, 0.39 mmol) and (4,5-dicarbomethoxy-1,3-dithiolyl)tributylphosphonium tetrafluoroborate (2.2 equivalents) in dry THF (15 mL) and triethylamine (0.6 mL). After subsequent work-up, the crude product was purified by silicagel column chromatography (methylene chloride) to afford (*Z* and *E*) **4a** as a dark red powder (152 mg, 60%). M.p. 201–203 °C; IR: $\tilde{\nu}_{max} = 1714$ cm^{-1} (C=O); ^{1}H NMR ($CDCl_3$): $\delta = 5.99$ (s, 4H) 3.83 (s, 12H); ^{13}C NMR ([D$_6$]DMSO): $\delta = 159.41$, 158.90, 130.64, 131.69, 131.36, 128.67, 117.33, 109.36, 107.89, 53.76, 53.13; MS (FAB+): *m/z*: 664 $[M]^+$.

2,6(7)-Bis(2,3-dimethyl-1,4-dithiafulven-6-yl)-TTF (4b): A solution of 4,5-dimethyl-1,3-dithiolium hexafluorophosphate (255 mg, 0.924 mmol), triphenylphosphine (244 mg, 0.924 mmol), and compound **10** (100 mg, 0.385 mmol) in a mixture of acetonitrile (8 mL) and THF (15 mL) was cooled at −80 °C under a nitrogen atmosphere. *n*-BuLi (1.6 M in hexanes, 0.53 mL, 0.847 mmol) was added dropwise and the resulting mixture was stirred at this temperature for 30 min. The mixture was then allowed to warm to RT and the precipitate thus formed was filtered and thoroughly washed with methanol, acetonitrile and diethyl ether to afford (*Z* and *E*) **4b** as a brown powder (112 mg, 60%). M.p. 182–185 °C; ^{1}H NMR ($CDCl_3$): $\delta = 5.95$ (s, 2H), 5.87 (s, 2H), 1.91 (s, 12H); MS (EI): *m/z* (%): 488 (35) $[M]^+$; MS (HRMS, EI): *m/z*: 487.8995; $C_{18}H_{16}S_8$ calcd 487.9018.

2,6(7)-Bis(2,3-bis(methoxycarbonyl)-1,4-dithiafulven-6-yl)-3,7(6)-bis(ethoxycarbonyl)-TTF (5a): Compound **5a** (method B) was synthesised by mixing the diformyl-TTF derivative **11** (63 mg, 0.16 mmol) and (4,5-dicarbomethoxy-1,3-dithiolyl)tributyl phosphonium tetrafluoroborate (2.2 equivalents) in THF (10 mL) and triethylamine (0.5 mL). The precipitate formed during the olefination reaction was filtered and thoroughly washed with methanol, acetonitrile and diethyl ether to afford (*Z* and *E*) **5a** as a very dark powder (red in solution) (113 mg, 90%). IR: $\tilde{\nu}_{max} = 1711$, 1692 cm^{-1} (C=O); UV/Vis (CH_2Cl_2): $\lambda_{max} = 525$ nm; ^{1}H NMR ($CDCl_3$/CS_2): $\delta = 7.63$ (s, 2H), 4.24 (q, 4H), 3.81 (s, 12H), 1.27 (t, 6H); MS (FAB+): *m/z*: 808 $[M]^+$; elemental analysis calcd (%) for $C_{28}H_{24}O_{12}S_8$: C 41.57, H 2.99, O 23.75, S 31.71; found C 41.01, H 3.05, O 23.48, S 30.98.

2,6(7)-(2,3-Dimethylsulfanyl-1,4-dithiafulven-6-yl)-3,7(6)-bis(ethoxycarbonyl)-TTF (5c): Compound **5c** (method A) was synthesised by starting from the diformyl-TTF derivative **11** (70 mg, 0.17 mmol). The precipitate formed during the olefination reaction was filtered and thoroughly washed with methanol, acetonitrile and diethyl ether to afford (*Z* and *E*) **5c** as a very dark powder (red in solution) (116 mg, 89%). IR: $\tilde{\nu}_{max} = 1680$ cm^{-1} (C=O); UV/Vis (CH_2Cl_2): $\lambda_{max} = 524$ nm; ^{1}H NMR ($CDCl_3$): $\delta = 7.66$ (s, 2H), 4.23 (q, 4H), 2.45 (brs, 12H), 1.30 (t, 6H); MS (FAB+): *m/z*: 760 $[M]^+$; elemental analysis calcd (%) for $C_{24}H_{24}O_4S_{12}$: C 37.86, H 3.18, S 50.55; found C 37.47, H 3.16, S 49.49.

2,6(7)-(1,4-Dithiafulven-6-yl)-3,7(6)-bis(ethoxycarbonyl)-TTF (5d): Compound **5d** (method A) was synthesised by starting from the diformyl-TTF derivative **11** (150 mg, 0.37 mmol). The precipitate formed during the olefination reaction was filtered and thoroughly washed with methanol, acetonitrile and diethyl ether to afford (*Z* and *E*) **5d** as a very dark powder (120 mg, 56%), sparingly soluble in most solvents. IR: $\tilde{\nu}_{max} = 1681$ cm^{-1} (C=O); UV/Vis (CH_2Cl_2): $\lambda_{max} = 513$ nm; MS (EI): *m/z* (%): 576 (28) $[M]^+$; elemental analysis calcd (%) for $C_{20}H_{16}O_4S_8$: C 41.64, H 2.80, O 11.09; found: C 41.45, H 3.02, O 10.83.

2,6(7)-Bis(2,3-bis(methoxycarbonyl)-1,4-dithiafulven-6-yl)-3,7(6)-dicyano-TTF (6a): Compound **6a** (method B) was synthesised by mixing the diformyl-TTF derivative **12** (60 mg, 0.19 mmol) and (4,5-dicarbomethoxy-1,3-dithiolyl)tributyl phosphonium tetrafluoroborate (2.2 equivalents) in THF (10 mL) and triethylamine (0.5 mL). Evaporation of the solvent under reduced pressure and addition of methanol resulted in precipitation of the product, which was filtered and thoroughly washed with methanol, acetonitrile and diethyl ether. Recrystallization from dichloromethane/methanol afforded (*Z* and *E*) **6a** as a very dark powder (97 mg, 70%). IR: $\tilde{\nu}_{max} = 2204$ (CN), 1714 cm^{-1} (C=O); UV/Vis (CH_2Cl_2): $\lambda_{max} = 493$ nm; MS (EI): *m/z* (%): 714 (51) $[M]^+$; elemental analysis calcd (%) for $C_{24}H_{14}N_2O_8S_8$: C 40.32, H 1.97, N 3.92, O 17.90, S 35.88; found C 40.18, H 2.00, N 3.96, O 17.82, S 35.07.

2,6(7)-(2,3-Dimethylsulfanyl-1,4-dithiafulven-6-yl)-3,7(6)-dicyano-TTF (6c): Compound **6c** (method A) was synthesised by starting from the diformyl-TTF derivative **12** (100 mg, 0.32 mmol). The precipitate formed during the olefination reaction was filtered and thoroughly washed with methanol, acetonitrile and diethyl ether, to afford (*Z* and *E*) **6c** as a very dark powder (149 mg, 70%); IR: $\tilde{\nu}_{max} = 2198$ cm^{-1} (CN); UV/Vis (CH_2Cl_2): $\lambda_{max} = 503$ nm; ^{1}H NMR ($CDCl_3$): $\delta = 6.59$ (s, 2H), 2.48 (s, 12H); MS (EI): *m/z* (%): 666 (84) $[M]^+$; elemental analysis calcd (%) for $C_{20}H_{14}N_2S_{12}$: C 36.01, H 2.11, N 4.19; found C 36.33, H 2.35, N 4.12.

2,6(7)-(1,4-Dithiafulven-6-yl)-3,7(6)-dicyano-TTF (6d): Compound **6d** (method A) was synthesised by starting from the diformyl-TTF derivative **12** (60 mg, 0.19 mmol). The precipitate formed during the olefination reaction was filtered and thoroughly washed with methanol, acetonitrile and diethyl ether to afford (*Z* and *E*) **6d** as a very dark powder (83 mg, 89%). IR: $\tilde{\nu}_{max} = 2193$ cm^{-1} (CN); UV/Vis (CH_2Cl_2): $\lambda_{max} = 480$ nm; MS (EI): *m/z* (%):482 (21) $[M]^+$; elemental analysis calcd (%) for $C_{16}H_6N_2S_8$: C 39.81, H 1.25, N 5.80; found C 39.20, H 1.55, N 5.62.

Formyl-TTF (7) and 2-formyl-6,7-(ethane-1,2-diyldisulfanyl)-TTF (8): These compounds were prepared following the described procedure, through lithiation (LDA/THF/−78 °C) and subsequent formylation of tetrathiafulvalene and (ethylenedithio)tetrathiafulvalene respectively, with Ph(Me)NCHO.[8, 9]

2-Formyl-6(7)-hydroxymethyl-TTF (9): A solution of equimolar amounts of 2,6(7)-bis(hydroxymethyl)-TTF[10] (200 mg, 0.75 mmol) and selenium dioxide (83 mg) was heated under reflux for 2 h in dry dioxane (20 mL); the solution turned from yellow to dark red. Cooling of the solution resulted in the formation of a black precipitate of elemental selenium, which was filtered and washed thoroughly with dichloromethane. The solvent mixture was then evaporated under reduced pressure to produce a dark red oil, which was purified by SiO_2 column chromatography (eluent: dichloromethane) to afford a first fraction, which corresponded to the 2,6(7)-diformyl TTF **10** (30 mg, 15%), and then as a second fraction the 2-formyl-6(7)-hydroxymethyl TTF **9** (CH_2Cl_2/Et_2O, 9:1) (80 mg, 40%). M.p. 162 °C; IR: $\tilde{\nu}_{max} = 3418$ (O–H), 1621 cm^{-1} (C=O); ^{1}H NMR ([D$_6$]DMSO): $\delta = 9.51$ (s, 1H), 8.24 (s, 1H, C*H*=CCHO), 6.58 (s, 1H), 5.55 (t, $J = 5.2$ Hz, 1H), 4.21 (d, $J = 5.2$ Hz, 2H); ^{13}C NMR ([D$_6$]DMSO): $\delta = 182.01$ (CHO), 143.59 (*C*=CCHO), 139.69 (*C*–CHO), 138.58 (*C*–CH_2), 114.75, 114.54 (*C*=C–CH_2OH), 105.23 (S_2C=CS_2), 58.90; MS (EI): *m/z* (%): 262 (100) $[M]^+$; MS (HRMS, EI): *m/z*: 261.9254; $C_8H_6O_2S_4$ calcd 261.9251.

2,6(7)-Diformyl-TTF (10): Propynal (CAUTION[14]) was generated by formolysis of propargylic diethylacetal synthesised according to ref. [13]. Treatment of propargylic diethylacetal (7.36 g, 160 mmol) with a large excess of formic acid previously dried over $CuSO_4$ for 3 h at RT resulted in the formation of propynal; the course of the reaction was monitored by ^{1}H NMR spectroscopy. The reaction mixture was then distilled under a very moderate vacuum; the condenser was connected to a $-30\,^\circ$C cooling stream. The fraction corresponding to $bp_{(0.9)} = 55-56\,^\circ$C was collected and analyzed by ^{1}H NMR. The mixture (3.10 g) was consisted of a 1:2 binary mixture of propynal/ethyl formiate and showed no presence of residual formic acid. A part of this mixture (0.30 g) was then directly added under nitrogen to a freshly distilled solution of $[Fe(\eta^2\text{-}CS_2)(CO)_2(PPh_3)_2]$[11] (2.13 g, 3 mmol) in toluene (60 mL). The red solution immmediately turned black. After stirring the solution for 0.2 h at RT, a solution of iodine (0.59 g) in toluene (20 mL) was added. After 4 h of stirring, the solvent was evaporated and the dark residue filtered over silicagel to discard undesirable inorganic salts. Purification by SiO_2 column chromatography (CH_2Cl_2) gave diformyl-TTF **10** as a purple powder (72 mg; 18% from propargylic aldehyde), for which all spectroscopic data were in accordance with literature.[10]

2,6(7)-Bis(ethoxycarbonyl)-3,7(6)-diformyl-TTF (11): A solution of dicobaltoctacarbonyl (1.09 g, 3.2 mmol) in toluene (15 mL) was added dropwise over 0.5 h (CO evolution), under nitrogen atmosphere, to a stirred solution of thione **18** (1.12 g, 4.8 mmol) in toluene (10 mL) at RT. The temperature was then raised to 40 °C for 0.5 h, and to was heated to reflux for 2 h. After cooling to RT, the reaction mixture was filtered over silicagel and elution was completed with dichloromethane in order to discard the black pyrophoric material. The solvent was then evaporated under reduced pressure, and the crude product thus obtained was recrystallised from dichloromethane/petroleum ether to afford a compound (*Z* and *E*) **11** as a deep blue powder (0.61 g, 63%). IR: $\tilde{\nu}_{max} = 1716$ (C=O ester), 1659 cm^{-1} (C=O aldehyde); UV/Vis (CH_2Cl_2): $\lambda_{max} = 581$ nm; ^{1}H NMR ($CDCl_3$): $\delta =$ 10.29 (s, 2H), 4.38 (q, 4H), 1.38 (t, 6H); ^{13}C NMR ($CDCl_3$): $\delta = 181.83$, 181.75, 158.2, 147.18, 146.95, 138.92, 138.86, 63.4, 14.03; MS (EI): *m*/*z* (%): 404 (100) $[M]^+$.

2,6(7)-Dicyano-3,7(6)-diformyl-TTF (12): A solution of the TTF derivative **20** (0.50 g, 1.1 mmol) in dichloromethane (20 mL) is treated at RT by formic acid (40 mL) for 0.20 h, the colour of the solution turning immediatly purple. Water (20 mL) was then added, and the resulting solution was extracted with dichloromethane. The organic layer was then washed with sodium carbonate (0.3 M) and water, dried ($MgSO_4$) and evaporated under reduced pressure, to produce a (*Z* and *E*) mixture of **12** as a black powder (0.32 g, 95%); IR: $\tilde{\nu}_{max} = 2223$ (CN), 1672 cm^{-1} (C=O); UV/Vis (CH_2Cl_2): λ_{max} 557 nm; ^{1}H NMR ($CDCl_3$): $\delta = 9.79$ (s, 2H); MS (EI): *m*/*z* (%): 310 (95) $[M]^+$.

4-Ethoxycarbonyl-5-diethoxymethyl-1,3-dithiole-2-thione (16): A solution of equimolar amounts of **14**[17b] (2.0 g, 10 mmol) and ethylenetrithiocarbonate (1.36 g) in freshly distilled xylene (10 mL) was heated under reflux for 24 h, after which solvent was removed under reduced pressure and the residue purified by chromatography over a silica column (toluene/hexane, 5:1). Thione **16** was isolated as a yellow oil which crystallised in the fridge (1.68 g, 54%). IR: $\tilde{\nu}_{max} = 1717$ (C=O), 1073 cm^{-1} (C=S); UV/Vis (CH_2Cl_2): $\lambda_{max} = 361$ nm; ^{1}H NMR ($CDCl_3$): $\delta = 6.14$ (s, 1H), 4.33 (q, 2H), 3.70 (br q, 4H), 1.36 (t, 3H), 1.26 (t, 6H); ES (EI): *m*/*z* (%): 308 (13) $[M]^+$, 263 (14), 218 (7), 103 (100).

4-Cyano-5-diethoxymethyl-1,3-dithiole-2-thione (17): A solution of equimolar amounts of **15**[17] (4.0 g, 26 mmol) and ethylenetrithiocarbonate (3.53 g) in freshly distilled xylene (20 mL) was heated under reflux for 8 h, after which solvent was removed under reduced pressure and the residue was purified by chromatography over a silica column (AcOEt/petroleum ether, 1:10). Thione **17** was isolated as a brownish oil, which crystallised in the fridge (5.31 g, 78%). IR: $\tilde{\nu}_{max} = 2220$ (CN), 1080 cm^{-1} (C=S); UV/Vis (CH_2Cl_2): $\lambda_{max} = 360$ nm; ^{1}H NMR ($CDCl_3$): $\delta = 5.56$ (s, 1H), 3.72 (br q, 4H), 1.26 (t, 6H); MS (EI): *m*/*z* (%): 261 (23) $[M]^+$, 216 (15), 103 (100).

4-Ethoxycarbonyl-5-formyl-1,3-dithiole-2-thione (18): A stirred solution of thione **16** (1.68 g, 5.45 mmol) in dichloromethane (30 mL) was treated by formic acid (100 mL) for 1 h. Water (100 mL) was then added, and the resulting solution was extracted with dichloromethane. The organic layer was then washed with sodium carbonate (0.3 mol L^{-1}) and water, dried ($MgSO_4$) and evaporated under reduced pressure. The residue was then purified by chromatography on a silica column (toluene), and recrystallised from dichloromethane/pentane to afford thin yellow needles of **18** (1.12 g, 88%). M.p. 30 °C; IR: $\tilde{\nu}_{max} = 1728$ (C=O ester), 1675 (C=O aldehyde), 1085 cm^{-1} (C=S); UV/Vis (CH_2Cl_2): λ_{max} 350 nm; ^{1}H NMR ($CDCl_3$): $\delta =$ 10.34 (s, 1H), 3.93 (q, 2H), 1.41 (t, 3H); MS (EI): *m*/*z* (%): 234 (100) $[M]^+$.

4-Cyano-5-formyl-1,3-dithiole-2-thione (19): A stirred solution of thione **17** (0.50 g, 15.4 mmol) in dichloromethane (60 mL) was treated by formic acid (50 mL) for 2 h. Water (100 mL) was then added, and the resulting solution was extracted with dichloromethane. The organic layer was then washed with sodium carbonate (0.3 mol L^{-1}) and water, dried ($MgSO_4$) and evaporated under reduced pressure. The residue was then purified by chromatography on a silica column (dichloromethane/petroleum ether, 2:1) to afford thione **19** as an orange powder (0.18 g, 50%). M.p. 92–94 °C; IR: $\tilde{\nu}_{max} = 2224$ (CN), 1665 (C=O), 1083 cm^{-1} (C=S); UV/Vis (CH_2Cl_2): λ_{max} 348 nm; ^{1}H NMR ($CDCl_3$): $\delta = 9.81$ (s, 1H).

2,6(7)-Dicyano-3,7(6)-bis(diethoxymethyl)-TTF (20): A solution of dicobaltoctacarbonyl (2.5 g, 7.4 mmol) in toluene (20 mL) was added dropwise over 0.5 h (CO evolution), under nitrogen atmosphere, to a stirred solution of thione **17** (2.93 g, 11 mmol) in toluene (20 mL) at RT. The temperature was then raised to 40 °C for 0.5 h, and heated to reflux for 1.5 h. After cooling to RT, the reaction mixture was filtered over silicagel and elution was completed with dichloromethane in order to discard the black pyrophoric material. The solvent was then evaporated under reduced pressure, and the crude product was purified by silicagel column chromatography (dichloromethane/petroleum ether, 1:1), to afford (*Z* and *E*) **20** as an orange powder (0.54 g, 21%). IR: $\tilde{\nu}_{max} = 2215$ cm^{-1} (CN); UV/Vis (CH_2Cl_2): λ_{max} 432 nm; ^{1}H NMR ($CDCl_3$): $\delta = 5.37$ (s, 2H), 3.69 (m, 8H), 1.28 (m, 12H); ^{13}C NMR ($CDCl_3$): $\delta = 154.5$, 110.4, 102.0, 97.4, 63.1, 14.9; MS (EI): *m*/*z* (%): 458 (26) $[M]^+$, 413 (17), 356 (19), 103 (100).

Acknowledgements

This work was supported by the following institutions: Ministère de l'Education Nationale (DRED), CNRS, Région des Pays de la Loire, Ville d'Angers, Département de Maine-et-Loire, as well by a financial support from CMEP 91 MDU167 which is gratefully acknowledged. Financial support from DGICYT under grants PB97-1186 and PB95-0428-C02-02 is also gratefully acknowledged by the groups at Zaragoza and Valencia, respectively. The group from Valencia thanks Dr. I. Tuñón for fruitful discussions on solvent calculations. Drs P. Cassoux and D. De Montauzon from the LCC of Toulouse are gratefully acknowledged for fruitful discussions and electrochemical experiments at ultramicroelectrode.

[1] J. M. Williams, J. R. Ferraro, R. J. Thorn, K. D. Carlson, U. Geiser, H. H. Wang, A. M. Kini, M. H. Whangbo, *Organic Superconductors (Including Fullerenes). Synthesis, Structure, Properties and Theory*, Prentice Hall, New Jersey, **1992**.

[2] For a reviews see: a) G. Saito, *Pure Appl. Chem.* **1987**, *59*, 999–1004; b) E. B. Yagubskii, *Mol. Cryst. Liq. Cryst.* **1993**, *230*, 631–648.

[3] a) M. Sallé, M. Jubault, A. Gorgues, K. Boubekeur, M. Fourmigué, P. Batail, E. Canadell, *Chem. Mater.* **1993**, *5*, 1196–1198; b) M. Sallé, A. Gorgues, M. Jubault, K. Boubekeur, P. Batail, R. Carlier, *Bull. Soc. Chim. Fr.* **1996**, *133*, 417–426.

[4] "Supramolecular Engineering of Synthetic Metallic Materials" A. Gorgues, M. Sallé, P. Hudhomme, P. Leriche, C. Boulle, C. Durand, F. Le Derf, M. Cariou, M. Jubault, P. Blanchard, in *NATO ASI Ser., Ser. C* (Eds.: J. Veciana, C. Rovira, D. B. Amabilino), Kluwer, Dordrecht, **1999**, *518*, pp. 451–466.

[5] a) J. Garín, J. Orduna, J. I. Rupérez, R. Alcalá, B. Villacampa, C. Sánchez, N. Martín, J. L. Segura, M. González, *Tetrahedron Lett.* **1998**, *39*, 3577–3580.

[6] M. Sato, N. G. Gonnella, M. P. Cava, *J. Org. Chem.* **1979**, *44*, 930–934.

[7] a) K. Ishikawa, K. Akiba, N. Inamoto, *Tetrahedron Lett.* **1976**, *17*, 3695–3698; b) K. Akiba, K. Ishikawa., N. Inamoto, *Synthesis* **1977**, 861–862; c) K. Akiba, K. Ishikawa., N. Inamoto, *Bull. Chem. Soc. Japan* **1978**, *51*, 2674–2683. For a detailed study of the Wittig olefination involving **W**, see also: d) J.-M. Fabre, L. Giral, A.

 © WILEY-VCH Verlag GmbH, D-69451 Weinheim, 2000 0947-6539/00/0607-1212 $ 17.50+.50/0

Gouasmia, H. J. Cristau, Y. Ribeill, *Bull. Soc. Chim. Fr.* **1987**, *5*, 823–826.
[8] a) D. C. Green, *J. Org. Chem.* **1979**, *44*, 1476–1479; b) J. Garín, J. Orduna, S. Uriel, A. J. Moore, M. R. Bryce, S. Wegener, D. S. Yufit, J. A. K. Howard, *Synthesis* **1994**, 489–493.
[9] K. Ikeda, K. Kawabata, K. Tanaka, M. Mizutani, *Synth. Met.* **1993**, *55–57*, 2007–2012.
[10] R. Andreu, J. Garín, J. Orduna, M. Savirón, J. Cousseau, A. Gorgues, V. Morisson, T. Nozdryn, J. Becher, R. P. Clausen, M. R. Bryce, P. Skabara, W. Dehaen, *Tetrahedron Lett*. **1994**, *35*, 9243–9246.
[11] H. Le Bozec, A. Gorgues, P. Dixneuf, *J. Am. Chem. Soc*. **1978**, *100*, 3946–3947.
[12] P. Leriche, A. Belyasmine, M. Sallé, P. Frère, A. Gorgues, A. Riou, M. Jubault, J. Orduna, J. Garín, *Tetrahedron Lett.* **1996**, *37*, 8861–8864.
[13] a) H. Le Bozec, A. Gorgues, P. Dixneuf, *Inorg. Chem.* **1981**, *20*, 2486–2489; b) A. J. Carty, P. Dixneuf, A. Gorgues, F. Hartstock, H. Le Bozec, N. J. Taylor, *Inorg. Chem.* **1981**, *20*, 3929–3934.
[14] a) J. C. Sheehan, J. A. Robinson, *J. Am. Chem. Soc*. **1949**, *71*, 1437; b) D. Makula, P. Lamy, *Acta Chim*. **1983**, *6*, 31–34.
[15] a) J. Garín, *Adv. Heterocyclic Chem.* **1995**, *62*, 249–304; b) G. Schukat, E. Fanghanel, *Sulfur Rep.* **1993**, *14*, 245–390.
[16] a) C. Bosshard, R. Speiter, P. Günter, R. R. Tykwinski, M. Schreiber, F. Diederich, *Adv. Mater.* **1996**, *8*, 231–234; b) H. S. Nalwa, T. Watanabe, S. Miyata, *Adv. Mater.* **1995**, *7*, 754–758.
[17] a) R. E. Murray, G. Zweifel, *Synthesis*, **1980**, 150.
[18] G. Le Coustumer, Y. Mollier, *J. Chem. Soc. Chem. Commun.* **1980**, 38–39.
[19] M. Sallé, A. Gorgues, M. Jubault, K. Boubekeur, P. Batail, *Tetrahedron* **1992**, *48*, 3081–3090.
[20] M. Sallé, A. J. Moore, M. R. Bryce, M. Jubault, *Tetrahedron Lett.* **1993**, *34*, 7475–7478.
[21] a) L. Huchet, S. Akoudad, E. Levillain, J. Roncali, A. Emge, P. Bauerle, *J. Phys. Chem. B*, **1998**, *102*, 7776–7781; b) J. B. Torrance, B. A. Scott, B. Welber, F. B. Kaufman, P. E. Seiden, *Phys. Rev. B* **1979**, *19*, 730–741; c) F. B. Kaufman, A. H. Schroeder, E. M. Engler, S. R. Kramer, J. Q. Chambers, *J. Am. Chem. Soc*. **1980**, *102*, 483–488; d) A. Smie, J. Heinze, *Angew. Chem.* **1997**, *109*, 375–379; *Angew. Chem. Int. Ed. Engl.* **1997**, *36*, 363–367; e) P. Tschuncky, J. Heinze, A. Smie, G. Engelmann, G. Kossmehl, *J. Electroanal. Chem.* **1997**, *433*, 223–226.
[22] a) A. Ohta, Y. Yamashita, *J. Chem. Soc. Chem. Commun*. **1995**, 557–558; b) A. Ohta, Y. Yamashita, *J. Chem. Soc. Chem. Commun*. **1995**, 1761–1762; c) P. Frère, A. Gorgues, M. Jubault, A. Riou, Y. Gouriou, J. Roncali, *Tetrahedron Lett*. **1994**, *35*, 1991–1994; d) A. Benahmed-Gasmi, P. Frère, J. Roncali, E. Elandaloussi, J. Orduna, J. Garín, M. Jubault, A. Gorgues, *Tetrahedron Lett*. **1995**, *36*, 2983–2986.
[23] Crystal data for compound **1a**: $C_{14}H_{10}O_4S_6$, monoclinic, $P2_1/c$, $Z=4$, $a=25.596(8)$, $b=5.345(2)$, $c=13.047(3)$ Å, $\beta=99.33(2)^\circ$, $V=1761(1)$ Å^3, $\lambda=0.71069$ Å. Data collection was carried out by the zig-zag $\omega/2\Theta$ scan technique $2^\circ \le \Theta \le 25^\circ$ on an Enraf-Nonius CAD4 diffractometer. Conditions of measurements were $t_{max}=40$ s, *hkl* range: $-30 \le h \le 30$; $0 \le k \le 6$; $0 \le l \le 15$. Intensity control reflections were measured every 2 h without appreciable decay (0.1%). A total of 2898 independent reflections were collected from which 2059 correspond to $I > 3\sigma(I)$. Structure refinement: After Lorentz and polarisation corrections, the structure was solved by direct methods (general tangent phasing procedure), which revealed all the non-hydrogen atoms. The structure was refined by full-matrix least-squares techniques (anisotropic refinement against F; x, y, z, U_{ij} for S, O and C atoms; 217 variables and 2059 observed reflections) with the resulting $R=0.048$ and $wR=0.056$. All the calculations were performed using the XTAL package.[47]
[24] a) N. Martín, L. Sánchez, C. Seoane, E. Ortí, P. M. Viruela, R. Viruela, *J. Org. Chem.* **1998**, *63*, 1268–1279; b) A. J. Moore, M. R. Bryce, A. S. Batsanov, A. Green, J. A. K. Howard, M. A. McKervey, P. McGuigan, I. Ledoux, E. Ortí, R. Viruela, P. M. Viruela, B. Tarbit, *J. Mater. Chem.* **1998**, *8*, 1173–1184.
[25] a) Y. Misaki, T. Sasali, T. Ohta, H. Fujiwara, T. Yamabe, *Adv. Mater.* **1996**, *8*, 804–807; b) A. Benahmed-Gasmi, P. Frère, E. H. El Andaloussi, J. Roncali, J. Orduna, J. Garín, M. Jubault, A. Riou, A. Gorgues, *Chem. Mater*. **1996**, *8*, 2291–2297; c) J. Roncali, L. Rasmussen, C. Thobie-Gautier, P. Frère, H. Brisset, M. Sallé, J. Becher, O. Simonsen, T. K. Hansen, A. Benahmed-Gasmi, J. Orduna, J. Garín, M. Jubault, A. Gorgues, *Adv. Mater.* **1994**, *6*, 841–845; d) H. Brisset, S. Le Moustarder, P. Blanchard, B. Illien, A. Riou, J. Orduna, J. Garín, J. Roncali, *J. Mater. Chem.* **1997**, *7*, 2027–2032; e) J. F. Favard, P. Frère, A. Riou, A. Benahmed-Gasmi, A. Gorgues, M. Jubault, J. Roncali, *J. Mater. Chem.* 1**998**, *8*, 363–366.
[26] R. S. Rowland, R. Taylor, *J. Phys. Chem.* **1996**, *100*, 7384–7391.
[27] a) C. Wang, M. R. Bryce, A. S. Batsanov, J. A. K. Howard, *Chem. Eur. J.* **1997**, *3*, 1679–1690; b) R. Viruela, P. M. Viruela, R. Pou-Amérigo, E. Ortí, *Synth. Met.* **1999**, *103*, 1991–1992.
[28] It was not possible to optimise the geometry of the radical cation of **1d** at the MP2 (UHF) level.
[29] P. M. Viruela, R. Viruela, E. Ortí, J. L. Brédas, *J. Am. Chem. Soc.* **1997**, *119*, 1360–1369.
[30] J. Fabian, B. A. Hess, Jr, *J. Org. Chem.* **1997**, *62*, 1766–1774.
[31] V. Schomaker, L. Pauling, *J. Am. Chem. Soc.* **1939**, *61*, 1769–1780.
[32] a) M. P. Cava, N. M. Pollack, G. A. Dieterle, *J. Am. Chem. Soc.* **1973**, *95*, 2558–2564; b) M. P. Cava, M. A. Sprecker, W. R. Hall, *J. Am. Chem. Soc.* **1974**, *96*, 1817–1821; c) T. Tsubouchi, N. Matsumura, H. Inoue, N. Hamasaki, S. Yoneda, Y. Kazunori, *J. Chem. Soc. Chem. Commun.* **1989**, 223–224; d) N. Beye, M. P. Cava, *J. Org. Chem.* **1994**, *59*, 2223–2226.
[33] a) M. R. Bryce, *J. Mater. Chem.* **1995**, *5*, 1481–1496; b) J. Roncali, *J. Mater. Chem.* **1997**, *7*, 2307–2321.
[34] B. Sahraoui, G. Rivoire, N. Terkia-Derdra, M. Sallé, J. Zaremba, *J. Opt. Soc. Am. B* **1998**, *15*, 923–928.
[35] a) M. Sylla, J. Zaremba, R. Chevalier, G. Rivoire, A. Khanous, A. Gorgues, *Synth. Metals* **1993**, *59*, 111–121; b) B. Sahraoui, M. Sylla, J. P. Bourdin, G. Rivoire, J. Zaremba, T. T. Nguyen, M. Sallé, *J. Modern Optics*, **1995**, *42*, 2095–2107.
[36] F. Gaillard, E. Levillain, *J. Electroanal. Chem.,* **1995**, *398*, 77–87.
[37] J. P. Perdew, *Phys. Rev. B* **1986**, *33*, 8822–8824.
[38] P. C. Hariharan, J. A. Pople, *Chem. Phys. Lett.* **1972**, *16*, 217–219.
[39] J. A. Pople, R. K. Nesbet, *J. Chem. Phys.* **1954**, *22*, 571–572.
[40] H. B. Schlegel, *J. Comput. Chem.* **1982**, *3*, 214–218.
[41] M. J. Frisch, G. W. Trucks, H. B. Schlegel, P. M. W. Gil, B. G. Johnson, M. A. Robb, J. R. Cheeseman, T. Keith, G. A. Petersson, J. A. Montgomery, K. Raghavachari, M. A. Al-Laham, V. G. Zakrzewski, J. V. Ortiz, J. B. Foresman, J. Cioslowski, B. B. Stefanov, A. Nanayakkara, M. Challacombe, C. Y. Peng, P. Y. Ayala, W. Chen, M. W. Wong, J. L. Andres, E. S. Replogle, R. Gomperts, R. L. Martin, D. J. Fox, J. S. Binkley, D. J. Defrees, J. Baker, J. P. Stewart, M. Head-Gordon, C. Gonzalez, J. A. Pople, *Gaussian 94, Revision B.1*, Gaussian, Pittsburgh PA, **1995**.
[42] J. J. P. Stewart, *J. Comput. Chem.* **1989**, *10*, 209–220; J. J. P. Stewart, *J. Comput. Chem.* **1989**, *10*, 221–264.
[43] A. Klamt, G. Shüürmann, *J. Chem. Soc. Perkin Trans. 2* **1993**, 799–805.
[44] *MOPAC93*, J. J. P. Stewart, Fujitsu, Tokyo, **1993**.
[45] J. Tomasi, M. Persico, *Chem. Rev.* **1994**, *94*, 2027–2094.
[46] In the case of compound **3a**, Wittig olefination was performed by generating **Wa** according to method A.
[47] S. R. Hall, H. D. Flack, J. M. Steward, *Xtal 3.4 Reference Manual*, Universities of western Australia, Geneva and Maryland, **1997**.

Received: July 12, 1999 [F1902]